



A layer stripping approach for monitoring resistivity variations using surface magnetotelluric responses



Xènia Ogaya^{a,b,*}, Juanjo Ledo^b, Pilar Queralt^b, Alan G. Jones^{a,1}, Álex Marcuello^b

^a Dublin Institute for Advanced Studies, School of Cosmic Physics, Dublin 2, Ireland

^b GEOMODELS Research Institute, Dept. Dinàmica de la Terra i de l'Oceà, Facultat de Geologia, Universitat de Barcelona, Barcelona, Spain

ARTICLE INFO

Article history:

Received 1 December 2015

Received in revised form 4 June 2016

Accepted 30 June 2016

Available online 4 July 2016

Keywords:

Magnetotellurics

Electromagnetic monitoring

Resistivity variations

Geological reservoirs

CO₂ storage sites

ABSTRACT

The resolution of surface-acquired magnetotelluric data is typically not sufficiently high enough in monitoring surveys to detect and quantify small resistivity variations produced within an anomalous structure at a given depth within the subsurface. To address this deficiency we present an approach, called “layer stripping”, based on the analytical solution of the one-dimensional magnetotelluric problem to enhance the sensitivity of surface magnetotelluric responses to such subtle subsurface temporal variations in resistivity within e.g. reservoirs. Given a well-known geoelectrical baseline model of a reservoir site, the layer stripping approach aims to remove the effect of the upper, unchanging structures in order to simulate the time-varying magnetotelluric responses at depth. This methodology is suggested for monitoring all kinds of reservoirs, e.g. hydrocarbons, gas, geothermal, compress air storage, etc., but here we focus on CO₂ geological storage. We study one-dimensional and three-dimensional resistivity variations in the reservoir layer and the feasibility of the method is appraised by evaluating the error of the approach and defining different detectability parameters. The geoelectrical baseline model of the Hontomín site (Spain) for CO₂ geological storage in a deep saline aquifer is taken as our exemplar for studying the validity of the 1D assumption in a real scenario. We conclude that layer stripping could help detect resistivity variations and locate them in the space, showing potential to also sense unforeseen resistivity variations at all depths. The proposed approach constitutes an innovative contribution to take greater advantage of surface magnetotelluric data and to use the method as a cost-effective permanent monitoring technique in suitable geoelectrical scenarios.

© 2016 Elsevier B.V. All rights reserved.

1. Introduction

The magnetotelluric (MT) method is not commonly used for monitoring studies because of its dependence on an uncontrolled and often (but not always) non-repeatable source that lowers the potential resolution of surface MT data compared to the resolution provided by other electromagnetic (EM) techniques. For this reason, EM monitoring studies are usually performed by means of direct-current (DC) (e.g. [Kiessling et al., 2010](#); [Bergmann et al., 2012](#)) and controlled-source EM (CSEM) methods (e.g. [Becken et al., 2010](#); [Girard et al., 2011](#); [Vilamajó et al., 2013](#); [Wagner et al., 2015](#); [Streich, 2016](#)) where the source is known and can be controlled. However, some attempts have been undertaken using the MT method for time-varying conductivity, especially over the last half-decade, in the following contexts:

(i) searching for earthquake precursory resistivity changes ([Park, 1996](#); [Svetov et al., 1997](#); [Sholpo, 2006](#); [Hanekop and Simpon, 2006](#); [Park et al., 2007](#); [Kappler et al., 2010](#)), (ii) in geothermal projects for studying the movement of fluids ([Pellerin et al., 1996](#); [Bedrosian et al., 2004](#); [Aizawa et al., 2011, 2013](#); [Peacock et al., 2012a,b, 2013](#); [MacFarlane et al., 2014](#); [Muñoz, 2014](#); [Rosas-Carbajal et al., 2015](#)), and (iii) in volcanic areas to investigate the relationship between EM pulses and type of eruption ([Aizawa et al., 2010](#)). In all of these cases, MT monitoring has been applied either by analyzing temporal variations in the electromagnetic spectra or by studying the evolution through time of the impedance tensor $Z_{ij}(\omega)$, the phase tensor, or directly, the MT responses (apparent resistivity and phase).

These above cited publications all show that resistivity variations are typically subtle and are usually difficult to detect and quantify using surface MT data because of the inherent resolution of the method. We propose a methodology based on the analytical solution of the one-dimensional (1D) MT problem to enhance the sensitivity capability of the surface MT responses. The objective is to remove the effects of the upper, unchanging, structures from the surface MT responses in order to obtain the pseudo-MT responses at the target depth, given a well-

* Corresponding author at: Dublin Institute for Advanced Studies, School of Cosmic Physics, 5 Merrion Square, Dublin 2, Ireland.

E-mail address: xogaya@cp.dias.ie (X. Ogaya).

¹ Now at: Complete MT Solutions, Ottawa, Canada.

known geoelectrical structure (baseline model). In this way, the technique (called “layer stripping” hereafter) can enhance sensitivity of surface data to small resistivity variations due to changes produced at the target depth (e.g. in the reservoir).

In a 1D Earth, the MT responses at depth only depend on the structures located below the observation point (i.e., they are independent of any layers located above it; Kaufman and Keller, 1981; Jones, 1983). However, in two-dimensional (2D) and three-dimensional (3D) settings the MT problem is more complex, because currents with deeper depth information flow both above and below the observation point, as discussed in Jones (1983) and Queralt et al. (2007). The layer stripping concept was already employed by Baba and Chave (2005) to eliminate 3D topographic effects from seafloor MT data, providing interesting results. Similarly, the concept was used in Queralt et al. (2007) to remove the responses of known 3D structures from the observed down-mine audio-magnetotelluric responses and, in this way, to enhance the sensitivity of below-mine potential ore bodies. In both cases, layer stripping was shown to be a useful tool to obtain approximate responses in a 3D Earth.

In this paper, the layer stripping method is further developed and presented as an approach to perform higher resolution EM monitoring using surface MT responses. We are aware of the limitations of the MT method, and, as the layer stripping approach works with surface MT data, the applicability of the suggested technique will be subjected to the same limitations. However, using this methodology we are able to highlight the changes observed in the surface data and better study the information contained therein. Thus, the layer stripping approach constitutes, from an economical point of view, an affordable permanent complementary monitoring technique to other financially or logistically more expensive and time-consuming options (such as CSEM or controlled-source seismology).

First we introduce the layer stripping method and validate it through synthetic studies (i) in 1D, to understand the methodology, and (ii) in 3D, to apply the method in a more realistic scenario. Although the approach can be applied for monitoring all kinds of reservoirs, e.g. hydrocarbons, gas, geothermal, compressed air storage, etc., in this paper we give physical meaning to these 1D and 3D resistivity variations assuming that they simulate CO₂ injections in a storage reservoir. The feasibility of the method is appraised evaluating the error of the approach and assessing its detecting ability defining a set of detectability parameters. Finally, the method is numerically tested in a real case study using the geoelectrical baseline model of the Hontomín CO₂ geological storage demonstration site in northwestern Spain (Ogaya et al., 2014). In this manner we appraise the validity of the 1D assumption on which the layer stripping approach is based using a real geoelectrical baseline model. Note that magnetotelluric responses expected on the surface and at depth were calculated using the 3D ModEM code of Egbert and Kelbert (2012).

2. The method: layer stripping

Resolution of time varying resistivity changes depends on the depth of the target, where shallower targets are resolved better than deeper targets. Based on that fact, the layer stripping methodology is proposed to increase the sensitivity of surface MT responses to resistivity variations produced at the *n*th-layer (layer in gray in Fig. 1) by removing the effect of the unchanging upper layers (from 1st-layer to (*n* – 1)th-layer; Fig. 1).

In a layered 1D Earth, the MT responses, both within the Earth and on the surface, can be derived using well-known analytical recursive relations (Srivastava, 1965; Patella, 1976; Kaufman and Keller, 1981; Ward and Hohmann, 1988; Grandis et al., 1999). The impedance at a given interface *Z_n* is derived from the impedance of the next deeper interface *Z_{n+1}* using an expression involving the frequency (ω , EM field characteristic) and the thickness and resistivity of the *n*th-layer (*h_n* and ρ_n , respectively; Fig. 1). Magnetic permeability is assumed to be the same for each layer (and to take the free space value), although

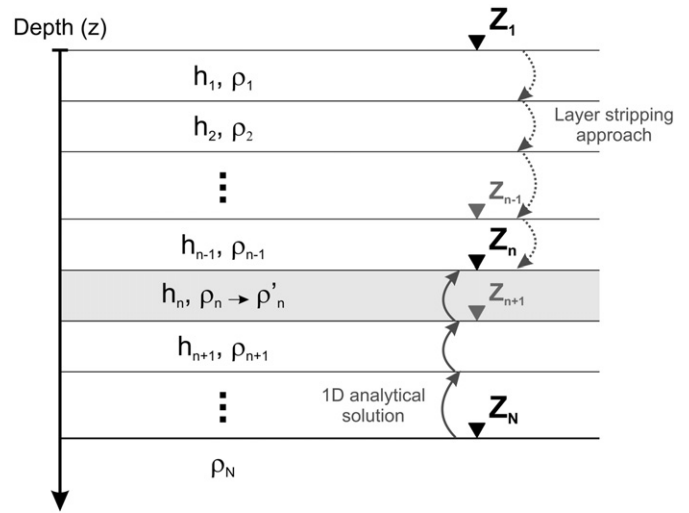


Fig. 1. N-layered 1D structure. *Z*₁ is the impedance tensor on the surface of the Earth and *Z_n*, the impedance tensor at top of the *n*th-layer. Each layer has a *h_n* thickness and a ρ_n resistivity. Resistivity changes from ρ_n to ρ'_n are located at the *n*th-layer (layer in gray). The stack of layers continues down to layer *N* which is a halfspace of resistivity ρ_N . The MT responses in 1D are computed using a recursive relation that goes from the bottom layer to the surface (Eq. (3) in the text). The proposed layer stripping approach moves downwards and computes the MT responses at a given depth starting with the MT responses on the surface (Eq. (4) in the text).

this could easily be modified if required, and the electric permittivity of each layer (i.e., the effects of displacement currents) is ignored.

Accordingly, first the impedance is determined at the top of the underlying homogenous halfspace *Z_N* (Fig. 1), denoted as layer *N*, viz.,

$$Z_N = \frac{\omega\mu}{k_N} \quad (1)$$

where *k_n* is the layer propagation constant within each layer and is given by

$$k_n = \sqrt{\frac{-i\omega\mu}{\rho_n}} \quad (2)$$

Moving upwards, the impedance tensor at the top of each layer is computed as follows (Srivastava, 1965 and Grandis et al., 1999):

$$Z_n = \frac{\omega\mu}{k_n} \coth \left[\cot h^{-1} \left(\frac{k_n Z_{n+1}}{\omega\mu} \right) + ih_n k_n \right]. \quad (3)$$

In this way, the impedance tensor *Z*₁ is calculated on the surface of the Earth (top of the layer 1, at *z* = 0).

The layer stripping approach is based on Eq. (3). Rewriting the equation, the inverse recursive relation allows us to move downwards and calculate responses at the top of the *n*th-layer from responses at the top of the (*n* – 1)th-layer. Thereby, the formulation for the layer stripping technique can be expressed as (Ogaya, 2014)

$$Z_n = \frac{\omega\mu}{k_{n-1}} \coth \left[\cot h^{-1} \left(\frac{k_{n-1} Z_{n-1}}{\omega\mu} \right) - ih_{n-1} k_{n-1} \right]. \quad (4)$$

Accordingly, *Z_n* is calculated from *Z*₁ using the known thickness and resistivity of each layer.

The error of the method can be estimated as a function of the surface impedance tensor Z_1 given the recursive relation shown in Eq. (4),

$$\delta|Z_n| = \left| \frac{1}{1 - \left(\frac{k_{n-1}Z_{n-1}}{\omega\mu}\right)^2} \left\{ -\csc h^2 \left[\cot h^{-1} \left(\frac{k_{n-1}Z_{n-1}}{\omega\mu} \right) - ih_{n-1}k_{n-1} \right] \right\} \right| \delta|Z_{n-1}|. \quad (5)$$

The surface data errors are assumed to be small, since good control of the noise contributions is required for monitoring purposes. In this way, a linear approximation of the error propagation is valid, as shown in Supplementary Fig. 1.

According to Eq. (5), the expressions of the error for the apparent resistivity (Ωm) and phase (degrees) are, respectively,

$$\delta\rho_{an} = \frac{2}{\omega\mu} |Z_n| \delta|Z_n| \quad (6)$$

and

$$\delta\varphi_n = \frac{180}{2\pi} \frac{1}{|Z_n|} \delta|Z_n|. \quad (7)$$

In real scenarios error is always present. For this reason, the impact of error on the layer stripping approach can be further examined defining a detectability parameter for each site and for each period, which will give us an estimate of the resistivity variations detectable in field experiments. Detectability is defined as the absolute value of the difference between the post-injection and pre-injection layer stripping solutions at a given depth divided by the quadratic addition of the pre-injection and post-injection errors of the layer stripping method at that depth. Thus, detectability for the absolute value of the impedance tensor $|Z|$ is defined as

$$D_{|Z|} = \frac{||Z_{post}| - |Z_{pre}||}{\sqrt{\varepsilon_{Z_{pre}}^2 + \varepsilon_{Z_{post}}^2}}. \quad (8)$$

Likewise, detectability of the real and imaginary parts of the impedance tensor Z is defined respectively, as

$$D_{\text{Real}(Z)} = \frac{|\text{Real}(Z_{post}) - \text{Real}(Z_{pre})|}{\sqrt{\varepsilon_{Z_{pre}}^2 + \varepsilon_{Z_{post}}^2}} \quad \text{and} \quad (9)$$

$$D_{\text{Imag}(Z)} = \frac{|\text{Imag}(Z_{post}) - \text{Imag}(Z_{pre})|}{\sqrt{\varepsilon_{Z_{pre}}^2 + \varepsilon_{Z_{post}}^2}}.$$

Similarly, the detectability of the apparent resistivity ρ_a and phase φ is defined by

$$D_{\text{App. Res.}} = \frac{|\rho_{apost} - \rho_{apre}|}{\sqrt{\varepsilon_{\rho_{apre}}^2 + \varepsilon_{\rho_{apost}}^2}} \quad \text{and} \quad D_{\text{Phase}} = \frac{|\varphi_{post} - \varphi_{pre}|}{\sqrt{\varepsilon_{\varphi_{pre}}^2 + \varepsilon_{\varphi_{post}}^2}}. \quad (10)$$

Hence detectabilities greater than one will represent differences between the pre-injection and post-injection state larger than the existing error, indicating detectable resistivity variations.

3. Synthetic data examples

The layer stripping approach is suggested for monitoring all kinds of reservoirs, and we take as our example CO_2 geological storage sites. We study the viability of the method defining a reference 1D model that reproduces the geoelectrical structure of a likely CO_2 storage site with electrical resistivities for the reservoir and seal layers similar to those observed at the Hontomín site (Ogaya et al., 2014; Fig. 2). We used a 1D model of seven layers in order to reproduce a realistic scenario: Layer 1 is a sedimentary cover of 60 Ωm . Layer 2 and Layer 4 are

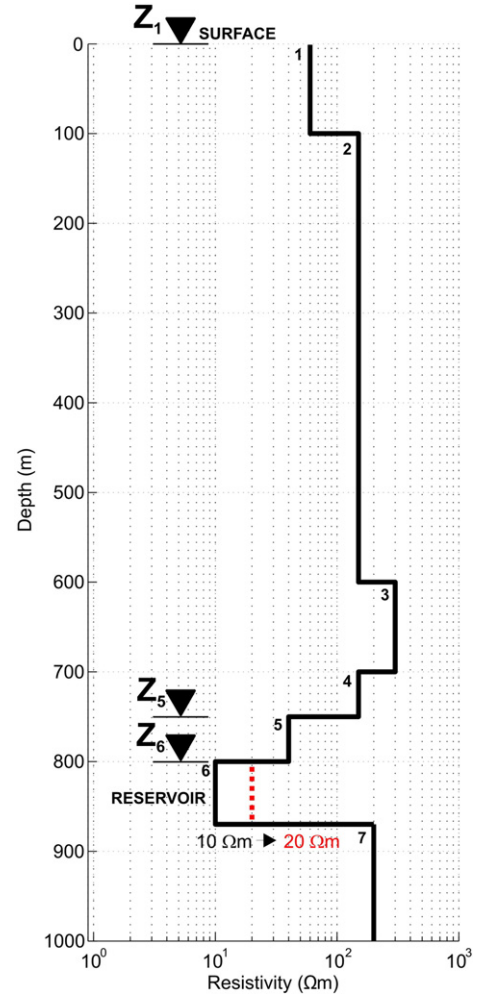


Fig. 2. One-dimensional resistivity model used for the synthetic studies. The resistivity model reproduces the geoelectrical structure of a likely CO_2 storage site. In order to simulate a CO_2 injection in 1D, the resistivity of the reservoir (6th-layer of the model) was modified from 10 Ωm to 20 Ωm assuming a saturation of 30%. Black triangles indicate the position of the MT measurements shown in Fig. 3.

siliciclastic layers of 150 Ωm (e.g., sandstones) with an interbedded Layer 3 of 300 Ωm (e.g., limestones). Layer 5 is a marly seal of 40 Ωm and Layer 6 is the target reservoir. The reservoir is located at 800 m depth – the minimum depth required for CO_2 geological storage (IPCC, 2005) – and is defined as a saline aquifer with an assigned resistivity of 10 Ωm . Finally, Layer 7 represents basement of 200 Ωm .

Archie's law (Archie, 1942) was used to estimate the expected increase in the reservoir resistivity in order to simulate the gas injection. In this way, the expected post-injection resistivity was determined to be twice the pre-injection resistivity, assuming clean sand in the reservoir (saturation exponent assumed equal to two) and a homogeneous CO_2 saturation of 30%. (We assume that the reservoir porosity does not vary as gas is injected.)

Thus, the layer stripping approach was applied to monitor resistivity variations from 10 Ωm to 20 Ωm in the reservoir. Two different monitoring scenarios were studied: (i) modifying the resistivity of the whole reservoir layer after injection (1D plume of CO_2) and (ii) placing 3D CO_2 plumes of different sizes in the reservoir layer (3D injection of CO_2).

3.1. One-dimensional resistivity variations

The layer stripping approach was applied to the 1D resistivity changes shown in Fig. 2 using Eq. (4). Fig. 3 shows the results at three

different depths: on the surface (Z_1), at the top of the seal layer (Z_5) and at the top of the reservoir layer (Z_6).

For 1D injection the layer stripping methodology predicts the same MT responses at depth as the ones provided by the analytical 1D solution (Fig. 3). Differences between the pre-injection and the post-injection state (i.e., resolution to resistivity changes) are observed to increase with the depth. Since the CO_2 layer is infinite in the two horizontal directions in the 1D case, resolution to resistivity changes is expected to be lower in either 2D or 3D injection scenarios, although charges on the boundaries may enhance sensitivity at some locations. In those 2D and 3D cases, the edge effects of the plume might not result in large changes comparable to those in 1D, as observed in e.g. Ogaya (2014).

3.1.1. Error propagation

Error of the stripping method was estimated as a function of the surface impedance Z_1 given that Z_n is a function of Z_1 (Eq. (5)). Since the method is proposed for monitoring surveys, we presume long time series are acquired and good control of the noise contributions is possible. In Fig. 3, a linear propagation of the error was performed (Eqs. (5), (6) and (7)) assuming an error of 1% of the surface impedance Z_1 on the data (1% of each impedance value). Noise levels in the data are appraised in further detail later on when evaluating the impact of the error on the detecting ability of the method. At the shortest periods (basically periods shorter than 10^{-2} s, i.e., frequencies higher than 100 Hz), the error is observed to increase significantly when removing the effects

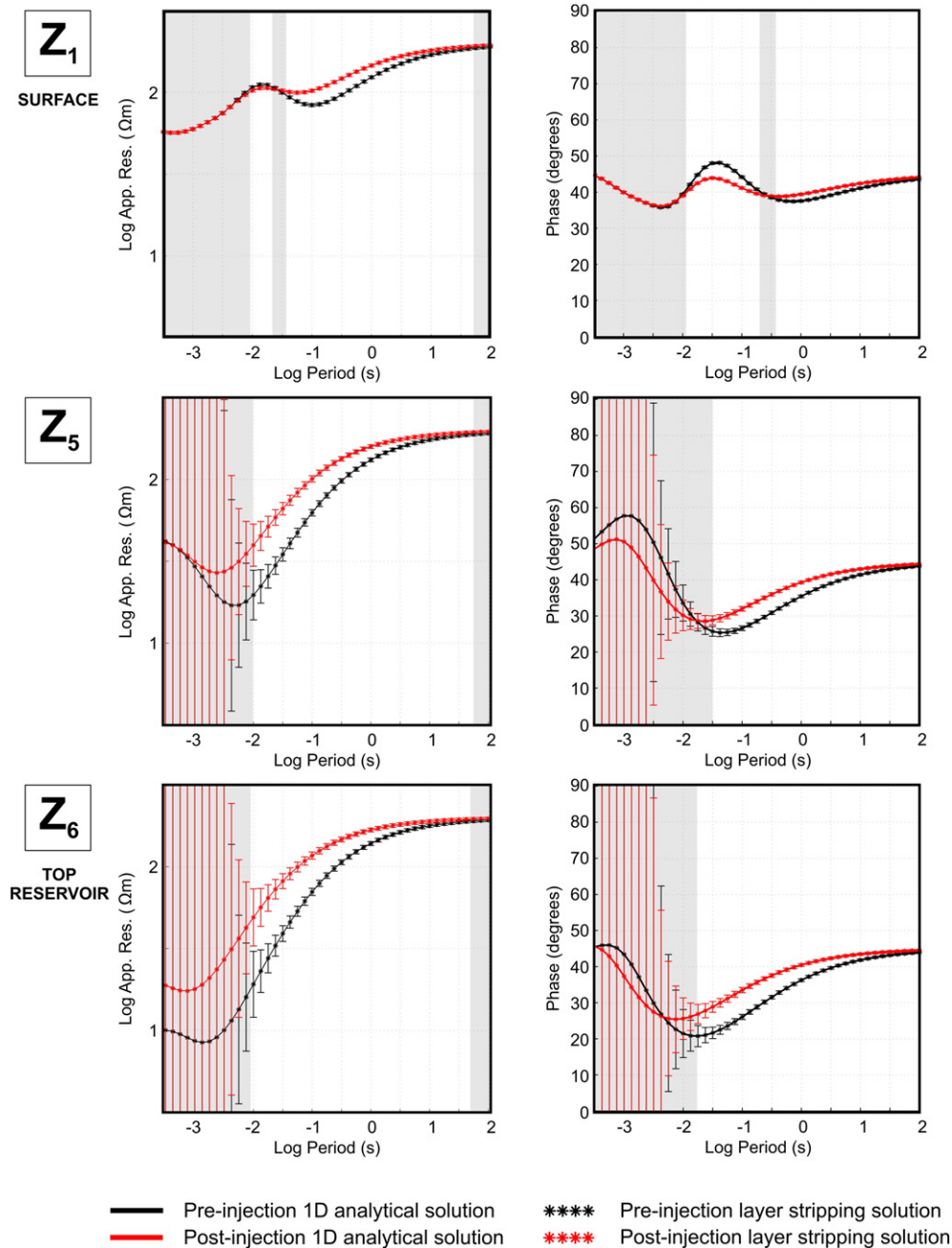


Fig. 3. Layer stripping results for 1D resistivity variations at three different positions: on the surface (Z_1), at the top of the 5th-layer (Z_5) and at the top of 6th-layer, the reservoir layer (Z_6). In black are displayed the responses of the pre-injection 1D model and in red, the responses of the post-injection 1D model (with CO_2). One-dimensional analytical solutions (Eq. (3) in the text) are plotted with continuous lines whereas the layer stripping results are plotted with small stars. Error assumed for the surface impedance tensor is 1% and insensitive periods (consequence of the error of the method, see Section 3.3) are partially masked.

of the upper layers (Fig. 3); this is essentially a consequence of attenuation and lack of deep penetration into the ground by high frequency data.

The effect of the number of removed layers on the error was studied comparing the stripping solution after removing the first layer of 60 Ωm and 100 m thickness (Fig. 4A) with the stripping solution after removing three different layers of 60 Ωm and a total thickness of 100 m (Fig. 4B). The error at the bottom of the layer (at 100 m depth - top of the underneath layer) is observed to be very similar in both cases. In the same way, the effect of the resistivity of the layer (stripped layer) was evaluated modifying the resistivity of the layer (first layer of the 1D model) to 10 Ωm (plotted in red in Fig. 4C) and to 300 Ωm (plotted in blue in Fig. 4C). The error associated with the removal of a conductive layer is demonstrated to be higher than the one associated with the removal

of a more resistive layer; this is due to far higher EM attenuation in conducting layers compared to resistive layers. Consequently, Fig. 4 shows that the error of the method depends on the electrical resistivity and thickness of the stripped layers (Fig. 4A, B and C), more correctly to their conductances (conductivity-thickness products), rather than on the number of layers removed (Fig. 4A and B).

3.1.2. Unforeseen resistivity variations

The layer stripping method aims to remove the effect of the unchanging layers from the post-injection MT responses, assuming that the resistivity changes are located at a known depth, i.e. in the reservoir layer. However, in real monitoring scenarios some unexpected resistivity changes could occur above the monitored layer, e.g. as a consequence of

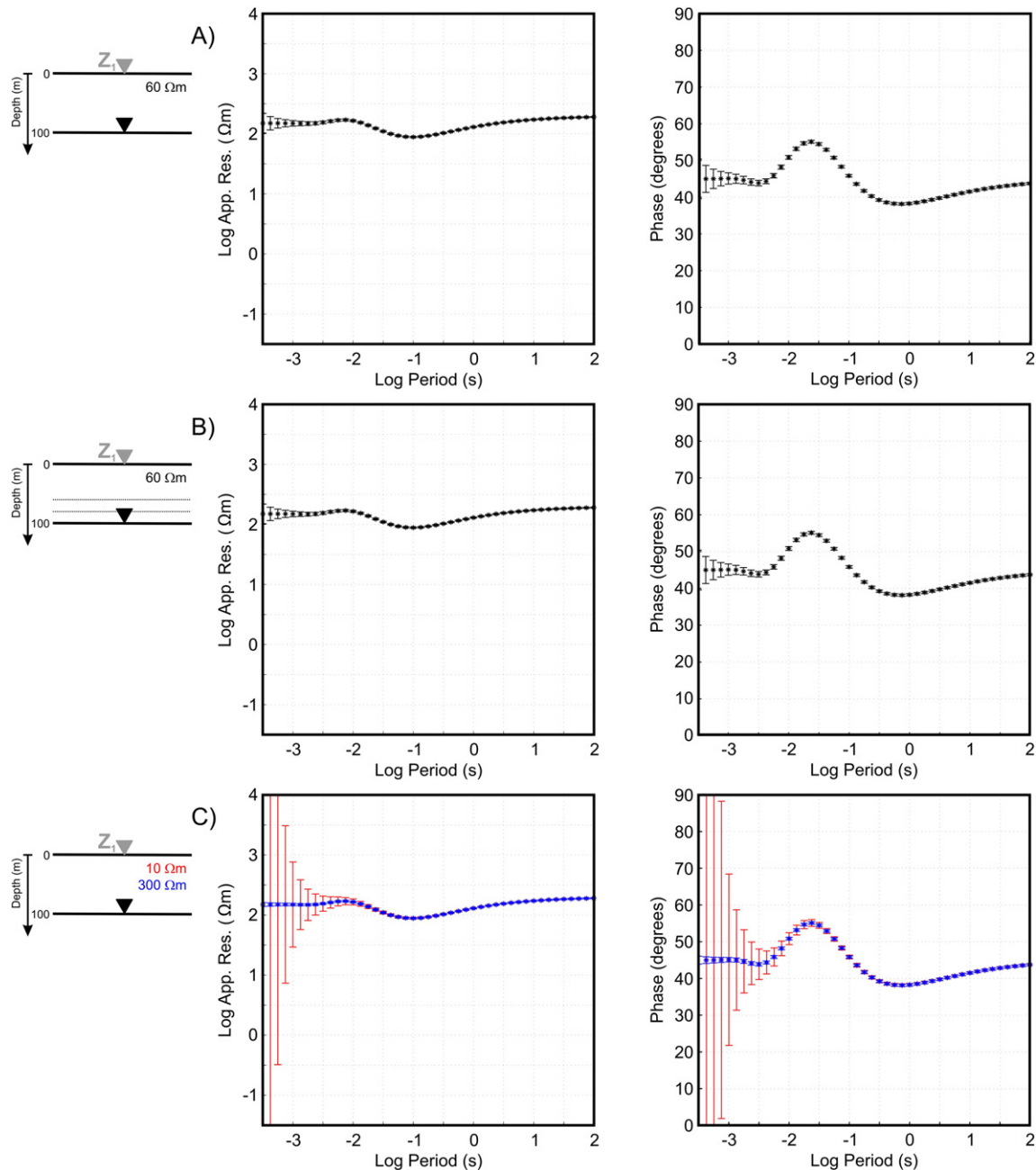


Fig. 4. Main characteristics of the error of the layer stripping method: A) Layer stripping results at 100 m depth after removing the effect of a single first layer of 60 Ωm and 100-m thick. B) Layer stripping results at 100 m depth after removing the effect of three layers of 60 Ωm and a total thickness of 100 m. C) Layer stripping results at 100 m depth after removing the effect of a single first layer of 100-m thick and 10 Ωm (in red) and of 100-m thick and 300 Ωm (in blue). Error assumed in all the cases for the surface impedance tensor is 1%.

unforeseen leakage, especially in the area surrounding the boreholes or along fractures. Consequently, we investigate how the proposed approach behaves when removing the effect of a layer that is not actually there. To do so, a more resistive layer of 300 Ωm and 100 m thick was introduced at 100 m depth (layer in red in Fig. 5A) – we doubled the resistivity of this layer to simulate a shallow injection (unforeseen leakage). The layer

stripping approach was then applied using the reference 1D model (model in black in Fig. 5A). Fig. 5 shows the results at four different depths: on the surface (Z_1 , Fig. 5B), at the top of the introduced resistive layer (Z_2 , Fig. 5C), at the bottom of the introduced resistive layer (Z_2' , Fig. 5D) and at the top of the 3rd-layer of the model (Z_3 , Fig. 5E). Layer stripping solutions for Z_2 display an offset between the pre-injection

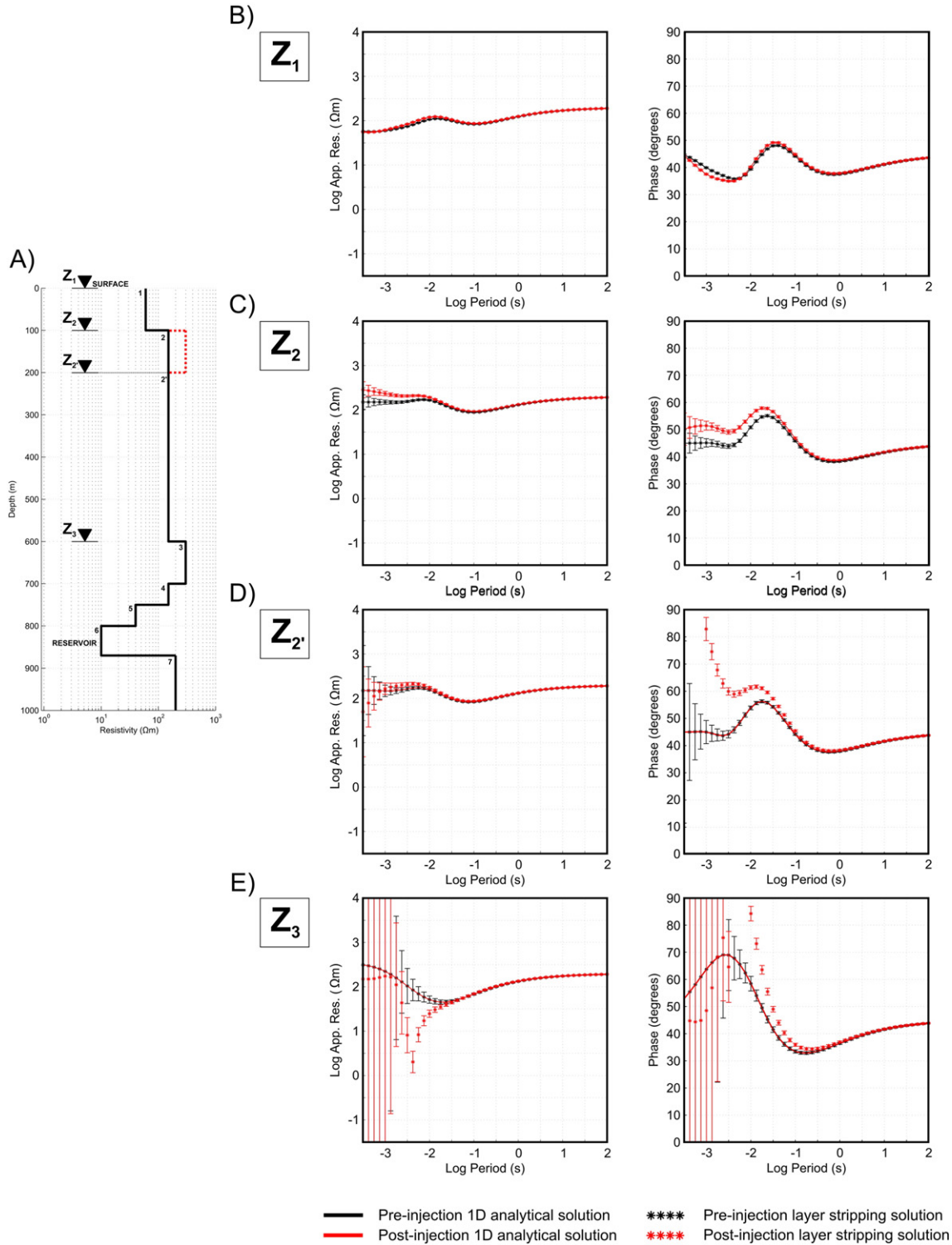


Fig. 5. Layer stripping results when removing a layer that is not actually there to simulate unexpected resistivity variations. A more resistive layer of 300 Ωm and 100-m thick was introduced at 100 m depth (A, in red). Layer stripping results were studied on the surface Z_1 (B), at the top of the introduced resistive layer Z_2 (C), at the bottom of the introduced resistive layer Z_2' (D) and at the top of the 3rd-layer Z_3 (E). Error assumed for the surface impedance tensor is 1%.

and the post-injection solutions obtained at the top of the introduced resistive layer. Thus, these results indicate that some resistivity changes are taking place at this depth. Moreover, if the effect of the next layer is removed without taking into account this offset, the layer stripping solution for Z_2 (Fig. 5D) is observed to present some inconsistencies in apparent resistivities and phases. These inconsistencies contain the effect of resistivity changes occurred in layer 2 of the model that have not been correctly removed. These inconsistencies propagate along the recursive stripping solutions computed at the top of the subsequent layers of the model (e.g. Z_3). Hence, the layer stripping approach will also facilitate detection of resistivity changes located at unexpected depths. However, it is important to note that this capability will be limited by the error of the method, which strongly depends on the geoelectrical structure of the study area (electrical resistivities and depths of interest).

3.1.3. Impact of subsurface heterogeneities

An important aspect to bear in mind when studying the viability of the layer stripping approach is that the near surface layers are inhomogeneous and these inhomogeneities are usually subject to time-lapse changes. Although seasonal variations could be evaluated during the characterization stage of the study site, a number of subsurface heterogeneities might remain unconstrained. For that reason, as a first approach to evaluate the impact of subsurface heterogeneities on the layer stripping approach, we scattered the 1D resistivity model shown in Fig. 2 with random resistivity variations of up to 10% in all cells of the model. Fig. 6 shows the impact of these subsurface heterogeneities on the surface and at the top of the reservoir.

The 1D model responses assuming an error of 1% are displayed in gray and the layer stripping solutions of the scattered model in black.

Subsurface heterogeneities generate a scattered layer stripping solution with a dispersion contained within the error of the approach, for an error of 1% assumed in the surface impedance tensor and a random resistivity variations of up to 10%. Thus, any small deviation from the stripped 1D baseline model, either because of cultural noise or subsurface time-lapse heterogeneities, will have the same kind of impact on the layer stripping solutions.

3.2. Three-dimensional resistivity variations

A more likely realistic monitoring scenario is simulated introducing 3D resistivity variations in the reservoir layer. A CO_2 plume of $1700 \times 1700 \times 70 \text{ m}^3$, which could represent an approximate volume of 3.8 Mt of CO_2 , was considered. The amount of CO_2 represented by this plume was estimated assuming a porosity of 12% for the reservoir and a homogeneous saturation of 30%. The CO_2 density at 800 m was considered to be 0.0038 times its density on the surface, according to IPCC (2005), for hydrostatic pressure and a geothermal gradient of $25 \text{ }^\circ\text{C}/\text{km}$ from $15 \text{ }^\circ\text{C}$ at the surface.

Fig. 7 shows the layer stripping solutions for the above mentioned resistivity variations on the surface (Z_1) and at the top of the reservoir (Z_6). For this 3D injection the layer stripping approach does not exactly recover the responses expected at the reservoir depth. However, from the results presented in Fig. 7 we can conclude that the method provides

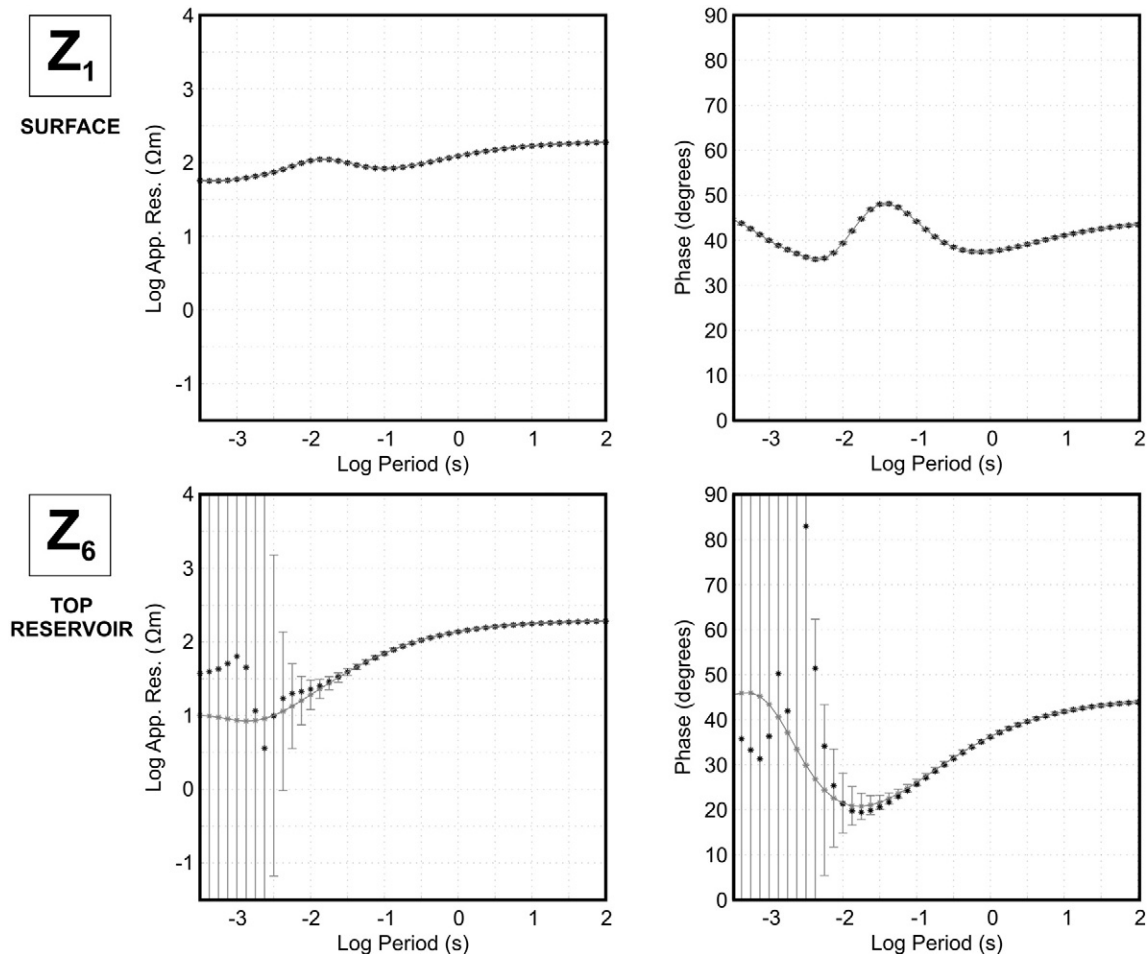


Fig. 6. Impact of subsurface heterogeneities. In gray, layer stripping results for 1D resistivity variations on the surface (Z_1) and at the top of 6th-layer, the reservoir layer (Z_6), assuming an error of 1% for the surface impedance tensor. Superimposed in black, layer stripping solutions for the same 1D model but scattered with random resistivity variations of up to 10%.

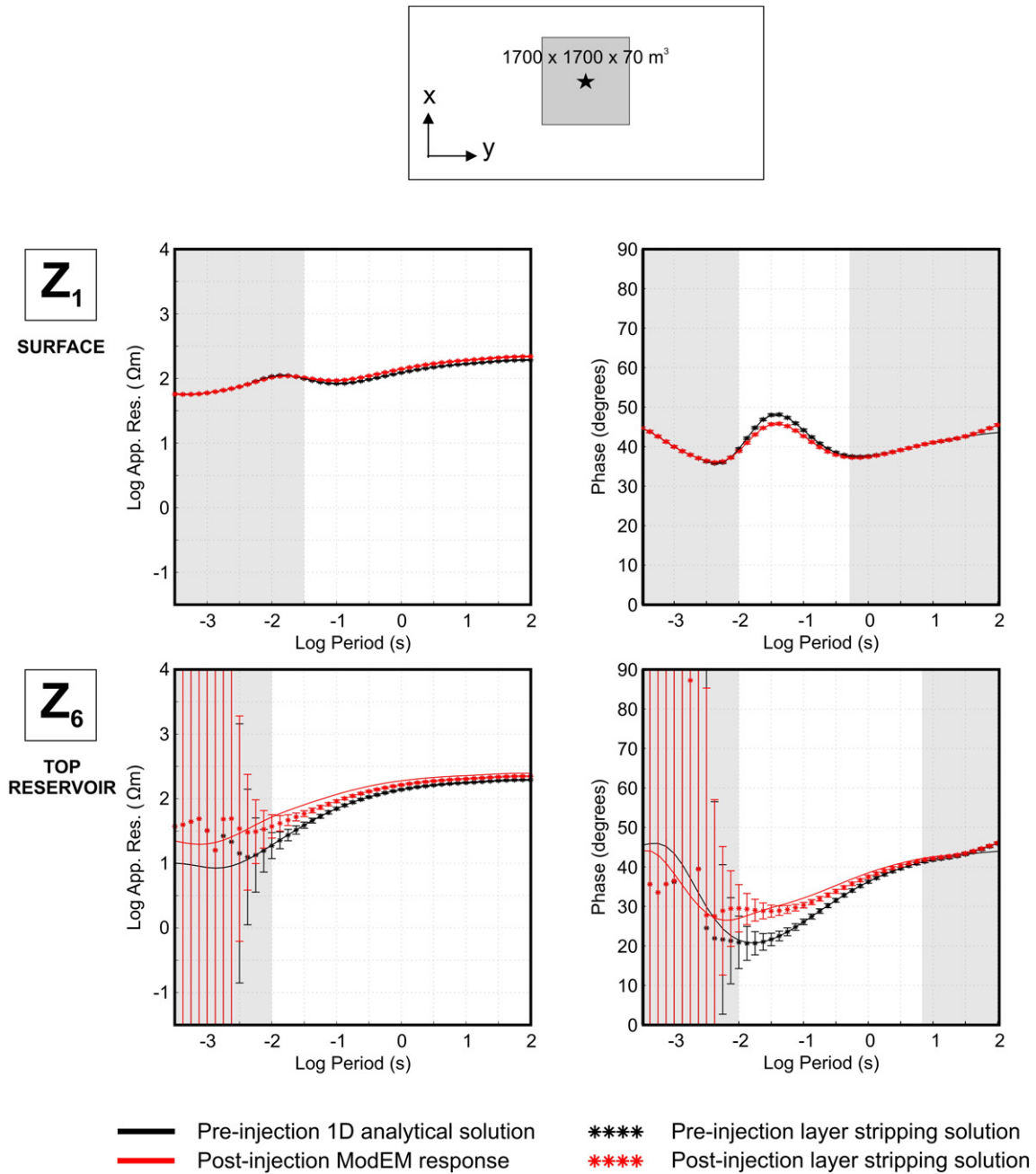


Fig. 7. Layer stripping results for a 3D plume of $1700 \times 1700 \times 70 \text{ m}^3$ and $20 \Omega\text{m}$ placed in the reservoir, at two different depths: on the surface (Z_1) and at the top of 6th-layer, the reservoir layer (Z_6). Responses are calculated at the center of the plume (black star); XY and YX polarizations are equal due to the symmetry of the problem. For the 3D case (post-injection case), the responses expected at depth were calculated using the ModEM code. Error assumed for the surface impedance tensor is 1% and insensitive periods (consequence of the error of the method, see Section 3.3) are partially masked.

good approximate responses. Thus, the proposed method is observed to facilitate enhanced variations for apparent resistivity and phase greater than the ones observed on the surface.

3.3. Detecting ability

The detectability parameters defined in Eqs. (8), (9) and (10) were used to evaluate the impact of the error on the layer stripping approach: Noise levels of 1%, 5% and 10% of the impedances were considered. Note that in all the following figures and in their corresponding explanation, impedance in 1D and impedance tensor in 3D (Z), apparent resistivity (ρ_a) and phase (φ) always make reference to the impedance (tensor), apparent resistivity and phase provided by the layer stripping approach.

Detectability values at the top of the different layers for the magnitude of the impedance tensor ($|Z|$), the real and imaginary parts of the impedance tensor, the apparent resistivity and the phase, are shown in Figs. 8 and 9 for the 3D plume studied previously ($1700 \times 1700 \times 70 \text{ m}^3$ and $20 \Omega\text{m}$) assuming an error of 1% for the surface impedance tensor.

Previous results have shown that the difference between the pre-injection and post-injection layer stripping solutions for the apparent resistivity and the phase at reservoir depth is greater than that obtained on the surface (Figs. 3 and 7). However, the detectability of $|Z|$ is not noticeably enhanced (Figs. 8A and 9A) because the error of the method also increases with depth (Fig. 7).

Figs. 8 and 9 also display the evolution of the detectability for the real and the imaginary parts of the impedance tensor (subfigures B and C, respectively) as stripping is applied. The imaginary part is observed to

be far more sensitive at depth than the real part (Figs. 8C and 9C). In contrast, the detectability for the real part of the impedance tensor is greater on the surface than at depth (Figs. 8B and 9B). This different evolution of the detectability of the real and imaginary parts of the impedance tensor with depth explains why the detectability of $|Z|$ remains practically constant at the top of the different layers. Whereas the detectability of the real part decreases with depth, the detectability of the imaginary part increases, making the detectability of the $|Z|$ nearly constant. Fig. 9C shows that the detectability of the imaginary part of the impedance tensor is maximum at the bottom of the reservoir.

Evolution of the detectability of apparent resistivity (Figs. 8D and 9D) is very similar to the evolution of the $|Z|$, as it was expected given the definition of the apparent resistivity ($\rho_a \propto |Z|^2$). However, evolution of the detectability of phase (Figs. 8E and 9E) clearly changes from one layer to another when applying the layer stripping technique. The results show that the changes observed at the top of the reservoir are located in a broader range of periods than the ones observed on the surface (Fig. 8E). Only the sites placed just above the plume sense more variations at the top of the reservoir (detectabilities above one) because of error propagation.

Figs. 8E and 9E highlight that the detectability of the phase is maximum when the responses are calculated at a depth below where the changes are taking place (in this case, below the reservoir layer). For this particular model, a strong peak is observed (Fig. 9E) after stripping a layer that is not actually there. This peak appears in all the sites located above or nearby the plume (Fig. 8E).

Thus, according to what was observed also in Fig. 5, for monitoring resistivity changes using the layer stripping technique it is important to pay particular attention to the evolution of the detectability of the imaginary part of the impedance tensor and to the evolution of the detectability of the phase in order to locate the changes not only at depth but also on the horizontal plane (delineate their limits).

For errors of 5% and 10% in the surface impedance tensor, only the detectabilities of the phases are above one (Fig. 10). (The evolution of all the detectability parameters is shown in Supplementary Figs. 2 and 3 for an error of 5% and in Supplementary Figs. 4 and 5 for an error of 10%). For an error of 10% (Fig. 10 and Supplementary Figs. 4 and 5), despite the resistivity variations are not observed on the surface, the resistivity changes are detected by the detectability of the phases at the bottom of the reservoir after applying the layer stripping approach. Thereby, the consistency of the layer stripping solutions at sites located along a profile may help to distinguish true resistivity variations from noise.

Simulating 3D plumes of different sizes and different noise levels we find that a minimum variation needs to be observed for resolution by the surface MT responses. Otherwise if the changes are not recorded in the surface acquired data, i.e. the response changes are below the noise level, the resistivity changes will not be enhanced by the layer stripping approach; obviously if there is no detectable signal in the surface data one will not be artificially created through layer stripping. Although thought, through precise and accurate removal of the overlying layers one may be able to sense spatially correlated signal over a band of frequencies that lies below the noise level for one frequency at an individual site that may be unrecognizable in the surface data (Fig. 10 and Supplementary Fig. 4).

Finally, we apply the layer stripping approach to a model that integrates all aspects studied above: the same 1D baseline model (Fig. 2) with one plume in the reservoir (as the previous studies) and a second plume at 500 m depth (bottom part of layer 2). The resistivity variations in the reservoir are from 10 Ω m to 20 Ω m and the size of these variations is 1.7 km \times 1.7 km \times 70 m. Upwards, the second plume has a volume of 1.7 km \times 1.7 km \times 100 m and represents variations from 150 Ω m to

300 Ω m. The post-injection model was scattered with random resistivity variations of up to 10% in all cells of the model to simulate subsurface heterogeneities. An error of 5% was assumed in the surface impedance tensor values. Detectabilities of the imaginary part of the impedance tensor and of the phases at different depth are shown in Fig. 11A and B, respectively. (See Supplementary Fig. 6 for all the detectability parameters). Whereas the detectability of all the components is close to one, only the detectability of the phase is above one (Fig. 11B). Some peaks are observed in the detectability of the phase at depths below where the resistivity changes are taking place: in dark blue, at the bottom of the second plume (the more resistive one) and in red, at the bottom of the reservoir layer. The detectability of the peak corresponding to the second plume is slightly below one whereas the peak corresponding to the reservoir plume is clearly above one (Fig. 11B). In reference to the detectability of the imaginary part of the impedance tensor (Fig. 11A), the maximum appears at the bottom of the reservoir layer. Thus, layer stripping enhances more the changes produced in the reservoir layer than the changes produced in layer 2. This is reasonable since surface MT data are more sensitive to changes produced in the reservoir (more conductive layer) than in layer 2 (more resistive). However, with errors slightly smaller than 5% on the surface data we would also be able to detect the shallower plume (layer 2).

Previously, we observed that the error associated with the removal of a conductive layer is greater than that associated with the removal of a more resistive layer of the same thickness (Fig. 4C). For this reason, the results obtained for the previous model were compared to those obtained for the same model but with an upper layer of 10 Ω m instead of 60 Ω m. Fig. 11C and D display the detectability of the imaginary part of the impedance tensor and the detectability of the phase, respectively. (The detectability of the rest of the components is shown in Supplementary Fig. 7). In general, all the detectabilities are lower than the ones observed for the same model but with an upper layer of 60 Ω m (Fig. 11A and B). Only the detectability of the phase at depths below the reservoir is above one (Fig. 11D) and the detectability of the imaginary part of the impedance tensor is maximum inside the reservoir (Fig. 11C). The existence of the second plume is difficult to detect in this model.

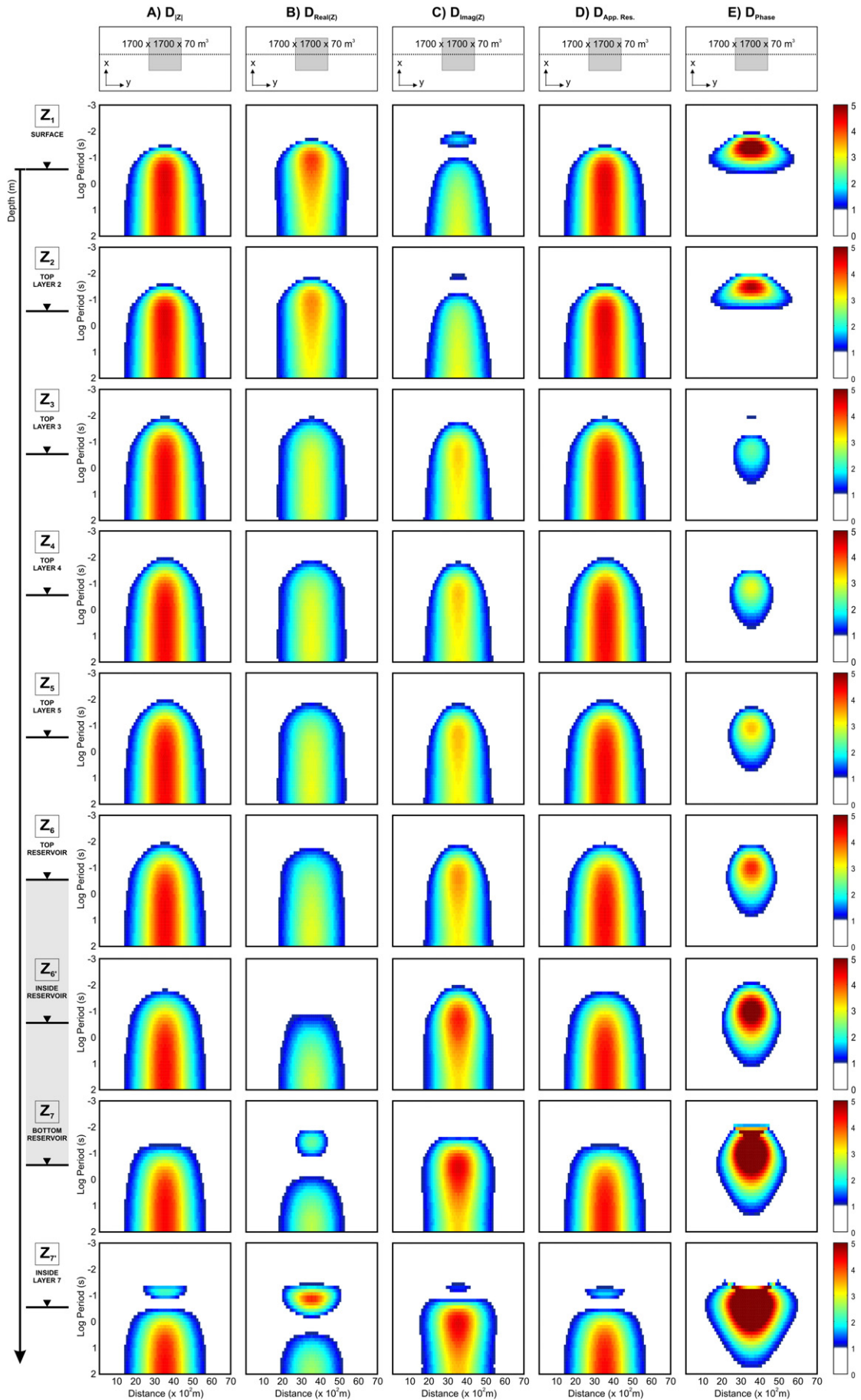
Therefore, sensitivity of the layer stripping approach to resistivity changes taking place in the subsurface depends primarily on the geoelectrical model itself, being limited by the resolution of the surface MT responses to these changes. All the examples studied demonstrate that the layer stripping might help to enhance the information contained in the surface data.

3.4. Case study: the Hontomín CO₂ storage site

The Hontomín site (Spain), established by Fundación Ciudad de la Energía (CIUDEN), is an Underground Research Laboratory (URL) for CO₂ geological storage in a deep saline aquifer. The primary reservoir has a thickness of more than 100 m and presents an average resistivity of 10 Ω m. The injection is projected into the basal part of a succession of Lower Jurassic carbonates at about 1500 m TVD (True Vertical Depth). See Ogaya (2014) for more details about the geoelectrical structure of the site.

A large number of multidisciplinary experiments were undertaken to characterize the subsurface and define the reference baseline models of the site (e.g. Rubio et al., 2011; Buil et al., 2012; Benjumea et al., 2012; Alcalde et al., 2013a, 2014; Canal et al., 2013; Elío, 2013; Nisi et al., 2013; Ogaya et al., 2013, 2014, 2016; Quintà, 2013; Ugalde et al., 2013; Vilamajó et al., 2013). Magnetotelluric characterization surveys provided the high-resolution 3D geoelectrical baseline model of the site (Ogaya,

Fig. 8. Detectability values at the top of all layers for the magnitude of the impedance tensor $|Z|$ (A), the real and imaginary parts of the Z (B and C, respectively), the apparent resistivity (D) and the phase (E) for a plume of 1700 \times 1700 \times 70 m³ and 20 Ω m. Detectabilities above one represent differences between the pre-injection and post-injection state higher than the existing error, indicating detectable resistivity variations. Error assumed for the surface impedance tensor is 1%.



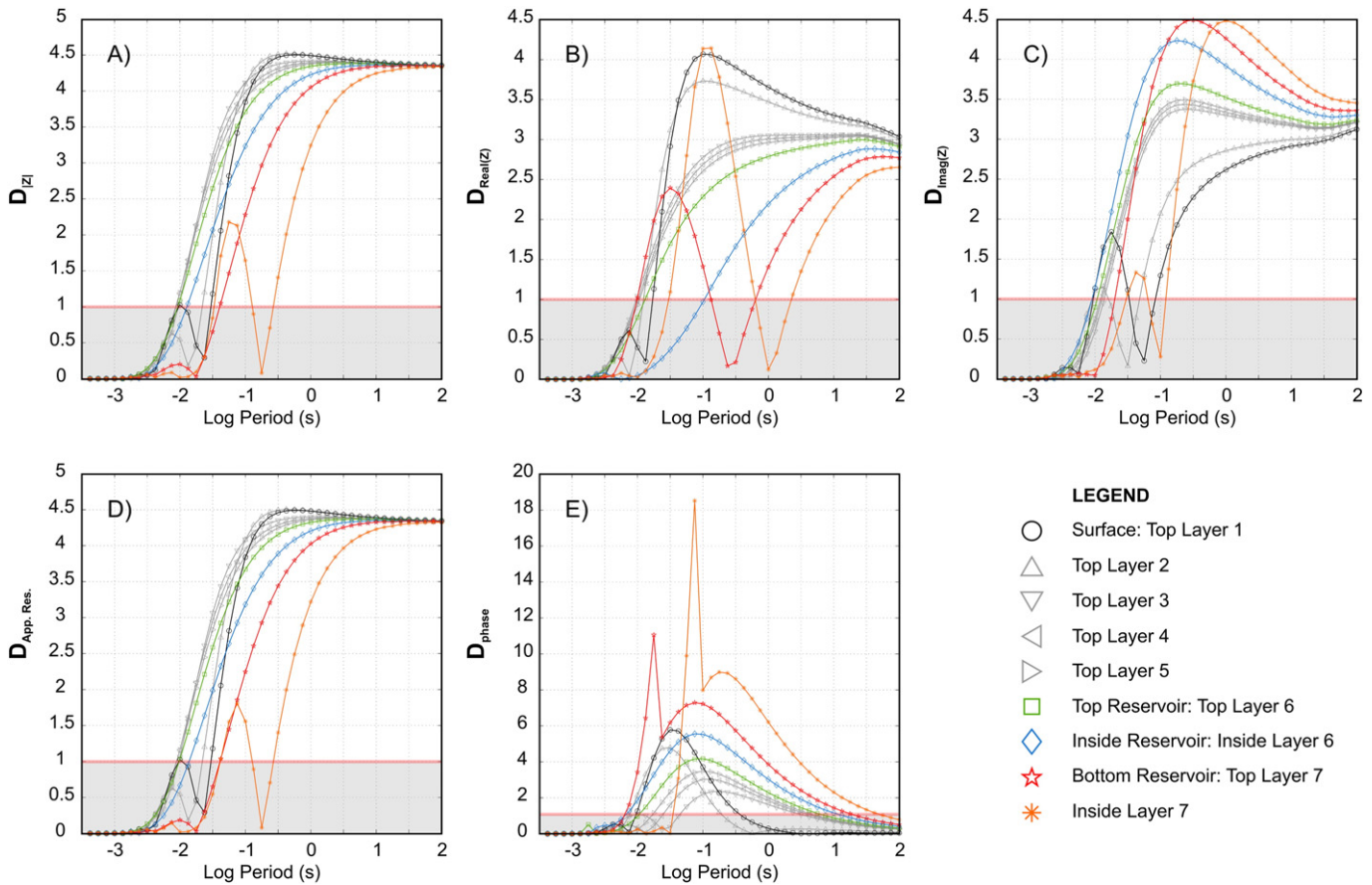


Fig. 9. Detectability values for a plume of $1700 \times 1700 \times 70 \text{ m}^3$ and $20 \Omega\text{m}$. Detectabilities are computed at the center of the plume and at the top of all layers for the magnitude of the impedance tensor $|Z|$ (A), the real and imaginary parts of the Z (B and C, respectively), the apparent resistivity (D) and the phase (E). The red line indicates detectability values equal to one. Detectabilities below one are partially masked in gray. Error assumed for the surface impedance tensor is 1%.

2014; Ogaya et al., 2014) that we employ here to test numerically the layer stripping methodology.

Synthetic studies using surface MT data and the geoelectrical baseline model of the site estimated that the minimum volume required to detect resistivity variations from $10 \Omega\text{m}$ to $40 \Omega\text{m}$ in the reservoir is $2200 \times 2200 \times 117 \text{ m}^3$ (Ogaya, 2014). This volume would represent a large amount of CO_2 . The reason such an amount is required is that

the geoelectrical structure of the study area and the depth at which the target reservoir is located do not constitute a favorable scenario for the MT method. A 1500-m depth resistive layer of around 100-m thickness (the expected injected gas) is hardly detectable by this EM technique, and would present severe logistical problems for CSEM methods besides the same sensitivity issues. However, although such a large amount of CO_2 is not planned for Hontomín, given the

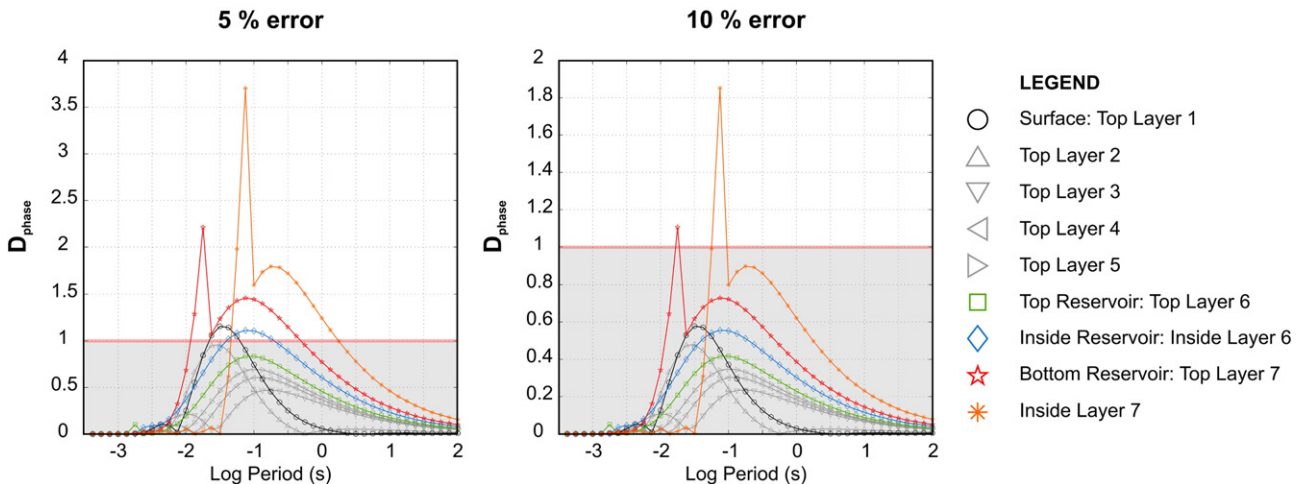


Fig. 10. Detectability of the phase at all depths for a plume of $1700 \times 1700 \times 70 \text{ m}^3$ and $20 \Omega\text{m}$, assuming an error of 5% and 10% for the surface impedance tensor. The red line indicates detectability values equal to one. Detectabilities below one are partially masked in gray.

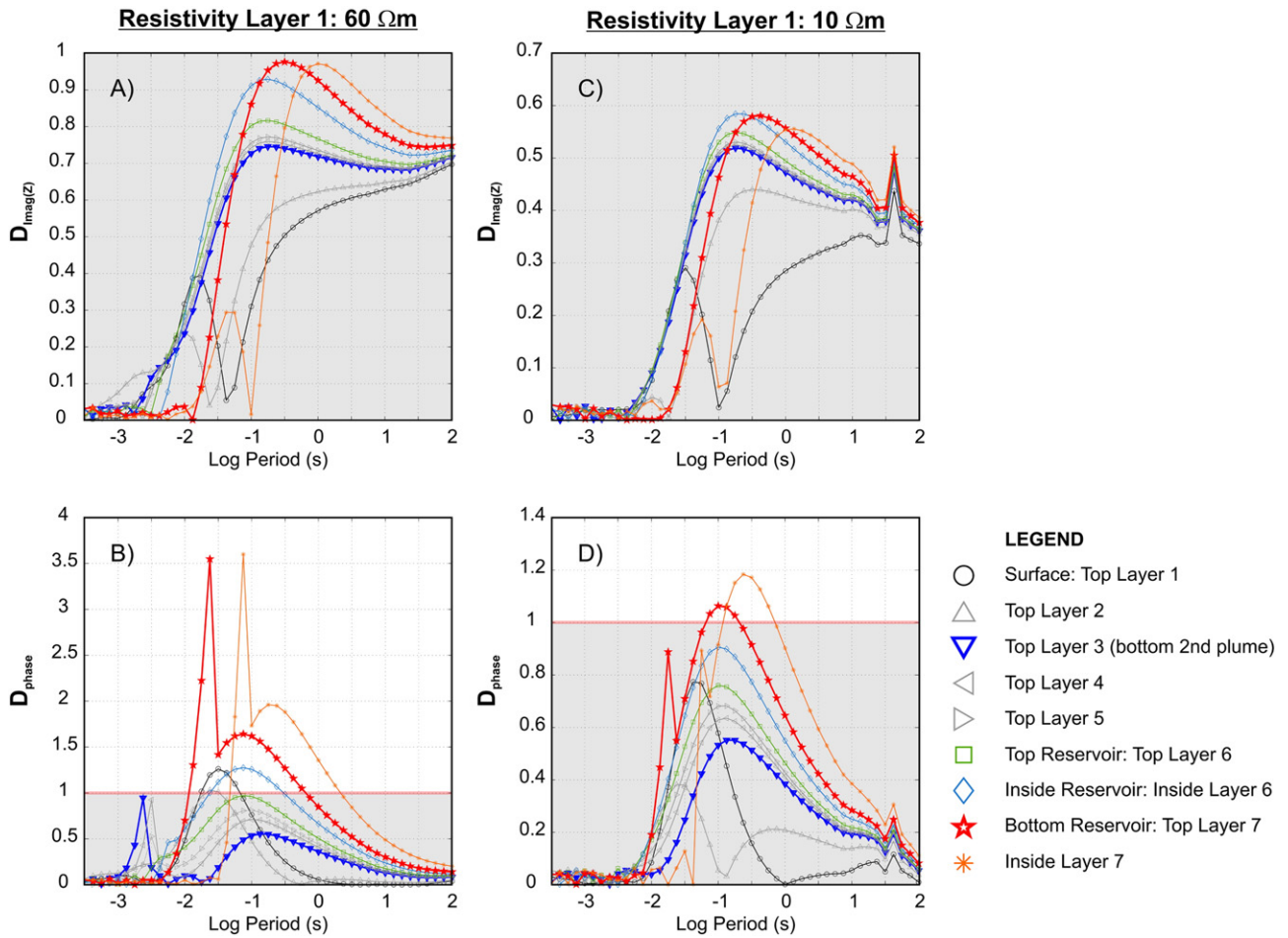


Fig. 11. Detectability of the imaginary part of the impedance tensor (A and C) and the phase (B and D) for two different models: the 1D baseline model (Fig. 2) with a first layer (layer 1) of 60 Ωm (A and B) and the 1D baseline model (Fig. 2) with a first layer (layer 1) of 10 Ωm (C and D). Both models have a plume of $1700 \times 1700 \times 70 \text{ m}^3$ and 20 Ωm in the reservoir layer and a second plume of $1700 \times 1700 \times 100 \text{ m}^3$ and 300 Ωm at 500 m depth (bottom layer 2). The post-injection models were scattered with random resistivity variations of up to 10% and an error of 5% was assumed for the surface impedance tensor. Detectabilities at the top of layer 3 (bottom of the second plume) are displayed in dark blue and detectabilities at the bottom of the reservoir layer, in red. The red line indicates detectability values equal to one. Detectabilities below one are partially masked in gray. The peak observed between 10^1 and 10^2 s in subfigures C and D is due to instabilities of the mesh.

dimensions of the site and the non-commercial, research character of the project, we use this CO_2 volume to test theoretically the layer stripping technique in a real scenario. The goal was to use a real geoelectrical baseline model to study if this methodology could be implemented in an actual monitoring survey, evaluating the validity of the 1D assumption on which the layer stripping approach is based and assessing how it would be possible to extract the baseline model from the post-injection responses in 3D environments. The impact of the error on the approach was extensively studied before and is not taken into account in this section.

First of all, the validity of the 1D assumption, and accordingly the validity of the layer stripping approach, was appraised by studying the influence of the medium located above the level of data acquisition. If the medium located above the reservoir affects the responses acquired at the reservoir depth to a great extent, then we cannot discard currents flowing above the observation level (i.e. the reservoir) and the 1D assumption on which the layer stripping approach is based, is not valid. With this aim, all layers overlying the reservoir were replaced by air-layers (i.e. layers of zero conductivity): Model A (Fig. 12) is the baseline model of the Hontomín site and model B (Fig. 12) is the baseline model with air-layers overlying the reservoir (bottom of the air layers at -408 m a.s.l. , approximate top of the reservoir). The MT responses that would be observed inside the reservoir (-478 m a.s.l.) at the injection well (Hi) location of both models are shown in Fig. 12. Electromagnetic characterization studies located the main reservoir-

seal system in the period range of 0.1 to 1 s (Ogaya et al., 2013) and, according to the dimensionality analysis of the acquired MT data, those periods displayed dominant 3D effects (Ogaya, 2014; Ogaya et al., 2014). However, Fig. 12 illustrates that the overlying air-layers do not affect responses inside the reservoir significantly, demonstrating the validity of performing a 1D layer stripping at the Hontomín site.

The effect of the upper layers was then removed from surface MT responses using our layer stripping technique. The 1D model provided by the column of the baseline 3D model located at Hi position (model called Hi model hereafter - in gray in Fig. 13A) did not fit either the XY or YX polarizations (Fig. 13B). Therefore, more suitable 1D models were sought for each polarization using the Hi model as a starting model. Thereby layer stripping was applied using the 1D models that best fit each polarization of the 3D model responses at Hi position (Fig. 13B).

The MT responses at the Hi well position were computed at two different depths (Fig. 14): at the surface, Z_S , and in the reservoir, Z_R (at -478 m a.s.l. , which means 1448 m TVD). Layer stripping results and responses predicted by the ModEM 3D forward code at both positions are shown in Fig. 14. Post-injection layer stripping solutions (red stars in Fig. 14) are scattered at some short periods, whereas the longest periods tend to overlap the pre-injection layer stripping solution (black stars) and are consistent with the ModEM responses. In general, as was observed above, the responses obtained by ModEM in the reservoir are not recovered by the layer stripping method. However, there is

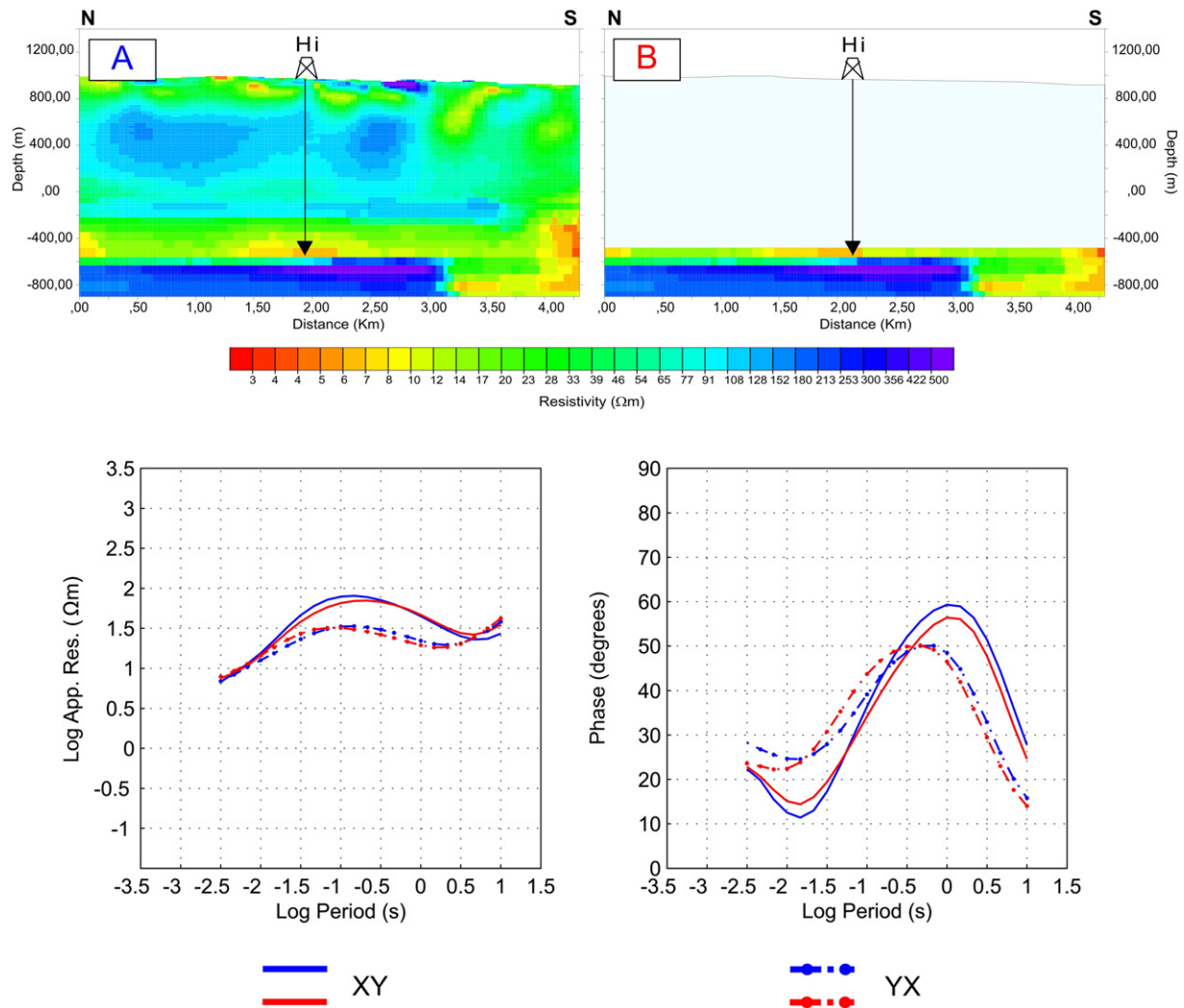


Fig. 12. Comparison of the MT responses inside the reservoir (at -478 m a.s.l.) between two models: model A is the geoelectrical baseline model of the Hontomín site (Ogaya et al., 2014) and model B is the baseline model with air layers overlying the reservoir. The bottom of the air layer is at -408 m a.s.l. Model A responses are plotted in blue, and model B responses are plotted in red. Continuous lines displayed XY polarization whereas dotted-dashed lines display YX polarization. Responses are calculated at the injection well (Hi) position.

improvement in the sensitivity of the MT responses to the resistivity changes produced in the reservoir.

Layer stripping results for the phases show greater differences between the pre-injection and post-injection state at reservoir depth for the YX polarization than for the XY polarization, despite greater variations observed in the surface data for XY polarization (1.6°) than for the YX polarization (1.1°). This might be due to the 1D models used in each case, and the small 2D and 3D effects observed at the reservoir level consequence of the medium located above the level of data acquisition (Fig. 12). The 1D models fit the surface MT responses with a maximum difference in the phases at the target periods (periods above 1 s) of 0.6° for XY polarization, and of 0.7° for the YX polarization, which means that we are not stripping away the models that completely fit the acquired surface responses. Moreover, 2D and 3D effects depart from the ideal 1D assumption, which entails that the layer stripping approach provides not exact but approximate response at depth.

4. Discussion

Previous studies report that the accuracy and precision of the surface MT responses are not typically sufficient for undertaking precise monitoring studies, as the MT method (as with all inductive EM methods) can be insensitive to changes produced by small resistivity variations

(e.g. Bedrosian et al., 2004; Aizawa et al., 2011; Peacock et al., 2012a,b, 2013). However, results presented in this paper show that our layer stripping approach is able to enhance the sensitivity of surface MT responses to the resistivity changes taking place at depth (e.g. in the reservoir). By removing the known layers, those layers are no longer variables so we are reducing the number of unknowns considerably. In other words, the layer stripping method removes the known time-invariant information from the acquired data and retains the time-varying information. In this way, time-lapse variations are isolated, being no longer masked by the MT responses of the unperturbed shallow structures.

The layer stripping concept is not new and has been utilized in different contexts in prior publications (e.g., Baba and Chave, 2005; Queralt et al., 2007). However, in this work the concept was further developed specifically for monitoring purposes. The main contribution of the formulation presented here is that it allows obtaining more accurate results than the previous approaches, since only the effect of the upper layers, not affected by the fluid injection, is removed. In previous studies the surface impedance tensor Z_1 was defined as $Z_1 = Z_{1n}Z_n$ where Z_{1n} included the MT responses of the layers comprised between the surface and the top of the n th-layer and Z_n was the MT response on the top of the n th-layer. In our development we do not use this formulation because both Z_{1n} and Z_n will be affected by resistivity variations

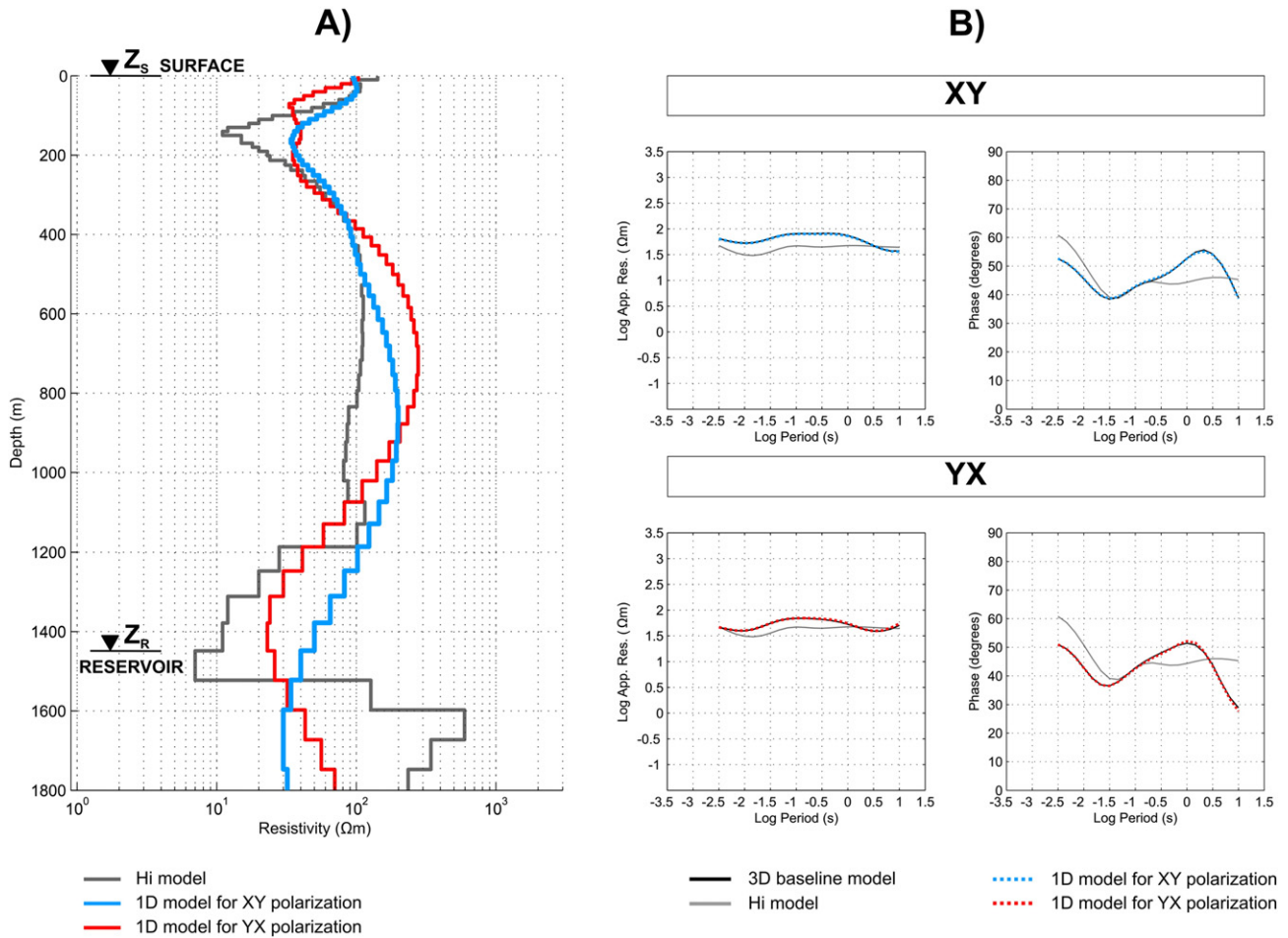


Fig. 13. A) One-dimensional model provided by the column of the 3D baseline model of Hontomín at Hi position -Hi model- (in gray) and the 1D models that best fitted XY and YX polarizations of the 3D baseline model at Hi well position (in blue and red, respectively). For the layer stripping, the MT responses were calculated on the surface (Z_s) and in the reservoir (Z_R). B) Magnetotelluric responses of the 3D geoelectrical baseline model at Hi position (in black), the Hi model (in gray) and the 1D models that best fitted XY and YX polarizations of the 3D model (in blue and red, respectively).

produced in the *n*th-layer (see Eq. (3)). Accordingly, stripping of Z_{1n} would also remove part of the effect of the fluid injection. The formulation suggested in this work (Eq. (4)) is more suitable for monitoring purposes because it facilitates removing only the effect of the upper layers not affected by the injection of fluid and thus totally recovers, to within experimental error, the effect of the injected fluid in 1D.

The effect of the noise on the approach has been comprehensively analyzed in this work. Data noise, which can be reduced with long time series and robust data processing techniques, can be overcome thereby applying the layer stripping approach at more than a single site and studying the evolution of the estimated MT responses at the top of the different layers. On the other hand, noise associated with the geological structure and its departure from a 1D model can be minimized with a good geoelectrical baseline model of the site. A high-resolution 3D reference model of the study area facilitates assessment of the validity of the 1D assumption, understanding and quantifying the error made when the structure is geoelectrically more complex. The greater the control of the noise, the higher will be the enhanced sensitivity of the magnetotelluric responses to the resistivity changes (reaching the ideal 1D case).

Phase and imaginary curves are more sensitive to time-varying changes in the subsurface than apparent resistivity and real part curves. The reason can be found in the dispersion relations, which are fulfilled for 1D structures (Weidelt, 1972) and for the TM mode for 2D structures (Weidelt and Kaikkonen, 1994). These relations connect apparent

resistivity and phase curves, as well as real and imaginary part curves, through Hilbert transformation. The phase curve at a given period is mainly controlled by the slope (derivative) of the apparent resistivity curve at the same period (Weidelt, 1972), and this relationship forms the basis of the Rho + approach of Parker and Booker (1996). In the same way, the imaginary part at each period is a derivative of the real part at the same period (Marcuello et al., 2005), which forms the basis of the original D + approach of Parker (1980). Accordingly, since the resistivity time-varying changes in the subsurface modify the observed responses (i.e. the shape of the curves), the changes are more clearly observed when looking at their derivative, that is to say, the phase and imaginary part curves.

The layer stripping approach works with surface MT data and consequently, is limited by the resolution of these surface data. In this way, some geoelectrical structures would be more favorable to this technique than others. However, the examples studied highlight that the approach would improve our sensitivity to the observed resistivity changes.

5. Conclusions

The layer stripping approach is an innovative methodology based on the analytical solution of the 1D MT problem with the overarching objective being to remove the effects of the well-known overlying structures from the surface MT responses in order to enhance the sensitivity to resistivity changes produced at a given depth. Synthetic studies show

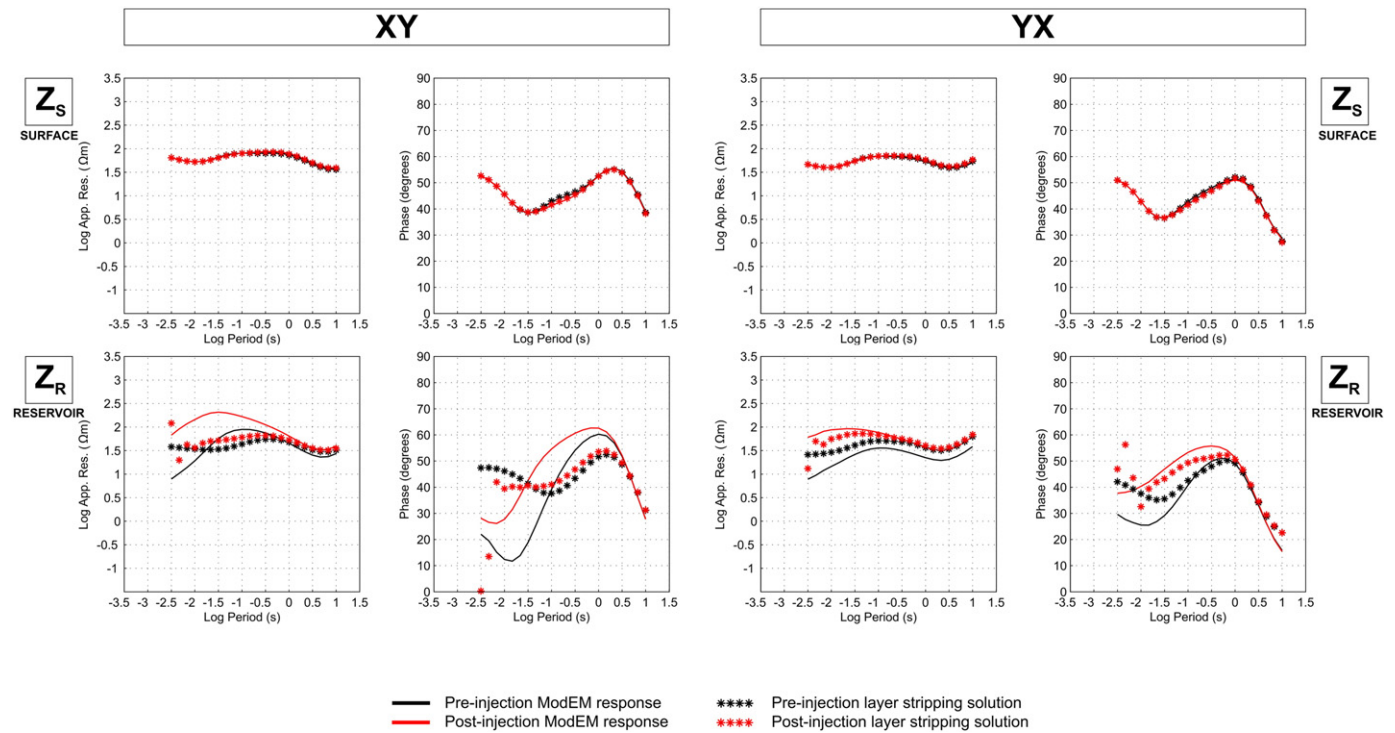


Fig. 14. Layer stripping results for a simulated CO₂ injection of 2200 × 2200 × 117 m³ and 40 Ωm at the Hontomín site. The MT responses are shown on the surface (Z_s) and in the reservoir (Z_r). ModEM responses are plotted with continuous lines whereas the layer stripping results are plotted with small stars.

that the approach provides the responses expected at depth for 1D resistivity changes, whereas for 3D resistivity variations it is not as exact as in 1D but provides valuable and useful approximate responses.

We conclude that the error of the method depends on the electrical resistivity and thickness of the stripped layers (more correctly, on their conductances) rather than on the number of layers removed. Moreover, the error associated with the removal of a conductive layer is observed to be higher than one associated with the removal of a more resistive layer; this makes intuitive sense given the difference in attenuation of signal between the two.

Despite the error, the results infer that detection of resistivity variations and localization of them in space (i.e. depth and lateral extent) is possible studying the evolution of not only the impedance tensors but also of the apparent resistivities and the phases at or in the different layers and along profiles/grids crossing the study area as stripping progresses. The phase and the imaginary part of the MT impedance tensor seem to be more sensitive to time-varying changes in the subsurface than the apparent resistivity and the real part. Besides, results show that phases are sensitive to the changes in a narrower range of periods than apparent resistivity, thus facilitating superior localization of the time-varying changes.

The method has been numerically tested in the Hontomín URL using the geoelectrical baseline model for the site. The outcomes indicate that the 1D assumption upon which the layer stripping approach is based would be valid in a real 3D scenario and that special care should be taken when seeking equivalent 1D models to apply the method to the surface data. The changes can be placed at incorrect depths if the conductance estimation (electrical conductivity and thickness product) is inaccurate.

The work presented here suggests that the layer stripping approach has the potential to be used in monitoring surveys to take greater advantage of the surface magnetotelluric data, making the method an affordable and logistically far simpler monitoring technique in suitable geoelectrical scenarios compared to controlled-source EM methods. Although the methodology has been numerically tested specifically for

CO₂ storage sites, the method is suggested for monitoring all kind of reservoirs. The layer stripping technique could sense not only expected resistivity variations in the reservoir layer but also detect unexpected resistivity changes at other depths.

Supplementary data to this article can be found online at <http://dx.doi.org/10.1016/j.jappgeo.2016.06.014>.

Acknowledgements

We wish to thank Professor Laust Pedersen for comments on the Ph.D. thesis of Ogaya, and the editor Dr. Jianghai Xia and two anonymous reviewers for their comments on the manuscript. XO is currently supported in DIAS by a Science Foundation Ireland grant IRECCSEM (SFI grant 12/IP/1313) awarded to AGJ. JL, PQ and AM thank Ministerio de Economía y Competitividad and EU Feder Funds through grant CGL2014-54118-C2-1-R. The authors would like to thank Gary Egbert and Anna Kelbert for providing the ModEM code, and the Irish Centre for High-End Computing (ICHEC) for providing the computing resources.

References

- Aizawa, K., Yokoo, A., Kanda, W., Ogawa, Y., Iguchi, M., 2010. Magnetotelluric pulses generated by volcanic lightning at Sakurajima volcano, Japan. *Geophys. Res. Lett.* 37, L17301. <http://dx.doi.org/10.1029/2010GL044208>.
- Aizawa, K., Kanda, W., Ogawa, Y., Iguchi, M., Yokoo, A., Yakiwara, H., Sugano, T., 2011. Temporal changes in electrical resistivity at Sakurajima volcano from continuous magnetotelluric observations. *J. Volcanol. Geotherm. Res.* 199, 165–175.
- Aizawa, K., Koyama, T., Uyeshima, M., Hase, H., Hashimoto, T., Kanda, W., Yoshimura, R., Utsugi, M., Ogawa, Y., Yamazaki, K., 2013. Magnetotelluric and temperature monitoring after the 2011 sub-Plinian eruptions of Shinmoe-dake volcano. *Earth Planets Space* 65, 539–550. <http://dx.doi.org/10.5047/eps.2013.05.008>.
- Alcalde, J., Martí, D., Calahorrano, A., Marzán, I., Ayarza, P., Carbonell, R., Juhlin, C., Pérez-Estaún, A., 2013a. Active seismic characterization experiments of the Hontomín research facility for geological storage of CO₂, Spain. *Int. J. Greenh. Gas Control* 19, 785–795. <http://dx.doi.org/10.1016/j.jggc.2013.01.039>.
- Alcalde, J., Marzán, I., Saura, E., Martí, D., Ayarza, P., Juhlin, C., Pérez-Estaún, A., Carbonell, R., 2014. 3D geological characterization of the Hontomín CO₂ storage site, Spain: multidisciplinary approach from seismic, well-logging and regional data. *Tectonophysics* 625, 6–25. <http://dx.doi.org/10.1016/j.tecto.2014.04.025>.

- Archie, G.E., 1942. The electrical resistivity log as an aid in determining some reservoir characteristics. *Trans. AIME* 146, 54–67.
- Baba, K., Chave, A., 2005. Correction of seafloor magnetotelluric data for topographic effects during inversion. *J. Geophys. Res.* 110, B12105. <http://dx.doi.org/10.1029/2004JB003463>.
- Becken, M., Streich, R., Krüger, K., Ritter, O., 2010. Exploration and monitoring of CO₂ storage sites using controlled-source electromagnetic: results of a feasibility study at Ketzin, Germany. XL385 EGU2010-7966, EGU General Assembly 2010.
- Bedrosian, P.A., Weckmann, U., Ritter, O., Hammer, C.U., Hübert, J., Jung, A., 2004. Electromagnetic monitoring of the Groß Schönebeck stimulation experiment. Presented at 64 Jahrestagung Der Deutschen Geophysikalischen Gesellschaft.
- Benjumea, B., Macau, A., Figueres, S., Gabàs, S., Sendra, R., Marzán, I., 2012. Testificación geofísica de Los Sondeos de investigación hidrogeológica de Hontomín (Burgos). IGC – Institut Geològic de Catalunya Technical Report, GA-002/12, Generalitat de Catalunya.
- Bergmann, P., Schmidt-Hattenberger, C., Kiessling, D., Rücker, C., Labitzke, T., Hennings, J., Baumann, G., Schütt, H., 2012. Surface-downhole electrical resistivity tomography applied to monitoring of CO₂ storage at Ketzin, Germany. *Geophysics* 77, B253–B267. <http://dx.doi.org/10.1190/geo2011-0515.1>.
- Buil, B., Gómez, P., Peña, J., Garralón, A., Galarza, C., Durán, J.M., Domínguez, R., Escribano, A., Turrero, M.J., Robredo, L.M., Sánchez, L., 2012. Caracterización Y monitorización hidrogeológica de Los acuíferos Superiores a la formación Almacenamiento de CO₂ (Hontomín, Burgos) Y actualización de la caracterización de Aguas Superficiales. Technical Report CIEMAT/DMA/2G010/1/2012.
- Canal, J., Delgado, J., Falcón, I., Yang, Q., Juncosa, R., Barrientos, V., 2013. Injection of CO₂-saturated water through a siliceous sandstone plug from the Hontomín test site (Spain): experiments and modeling. *Environ. Sci. Technol.* 47 (1), 159–167. <http://dx.doi.org/10.1021/es301222z>.
- Egbert, G.D., Kelbert, A., 2012. Computational recipes for EM inverse problems. *Geophys. J. Int.* 189 (1), 251–267. <http://dx.doi.org/10.1111/j.1365-246X.2011.05347.x>.
- Elio, J., 2013. Estrategias De monitorización de CO₂ Y Otros Gases en Los Estudios de análogos Naturales (PhD Thesis) Universidad Politécnica de Madrid.
- Girard, J.F., Coppo, N., Rohmer, J., Bourgeois, B., Naudet, V., Schmidt-Hattenberger, C., 2011. Time-lapse CSEM monitoring at Ketzin (Germany) CO₂ injection using 2xMAM configuration. *Energy Procedia* 4, 3322–3329.
- Grandis, H., Menvielle, M., Roussignol, M., 1999. Bayesian inversion with Markov chains-I. The magnetotelluric on-dimensional case. *Geophys. J. Int.* 138 (3), 757–768.
- Hanekop, O., Simpon, F., 2006. Error propagation in electromagnetic transfer functions: what role for the magnetotelluric method in detecting earthquake precursors? *Geophys. J. Int.* 165, 763–774. <http://dx.doi.org/10.1111/j.1365-246X.2006.02948.x>.
- IPCC – Intergovernmental Panel on Climate Change, 2005. IPCC Special Report on Carbon Dioxide Capture and Storage. Prepared by Working Group III of the Intergovernmental Panel on Climate Change [Metz, B., O. Davidson, H. C. de Coninck, M. Loos, and L. A. Meyer (Eds.)]. Cambridge University Press, Cambridge, United Kingdom and New York, NY, USA.
- Jones, A.G., 1983. A passive, natural-source, twin-purpose borehole technique: vertical gradient magnetometry (VGM). *J. Geomagn. Geoelectr.* 35, 473–490.
- Kappler, K.N., Frank Morrison, H., Egbert, G.D., 2010. Long-term monitoring of ULF electromagnetic fields at Parkfield, California. *J. Geophys. Res.* 115, B04406. <http://dx.doi.org/10.1029/2009JB006421>.
- Kaufman, A., Keller, G.V., 1981. The magnetotelluric sounding method. *Meth. Geochem. Geophys.* 15 (583 pp.).
- Kiessling, D., Schmidt-Hattenberger, C., Schuett, H., Schilling, F., Krueger, K., Schoebel, B., Danckwardt, E., Kummerow, J., CO₂SINK Group, 2010. Geoelectrical methods for monitoring geological CO₂ storage: first results from cross-hole and surface-downhole measurements from the CO₂SINK test site at Ketzin (Germany). *Int. J. Greenh. Gas Control* 4 (5), 816–826. <http://dx.doi.org/10.1016/j.ijggc.2010.05.001>.
- MacFarlane, J., Thiel, S., Pek, J., Peacock, J., Heinson, G., 2014. Characterisation of induced fracture networks within an enhanced geothermal system using anisotropic electromagnetic modelling. *J. Volcanol. Geotherm. Res.* 288, 1–7. <http://dx.doi.org/10.1016/j.jvolgeores.2014.10.002>.
- Marcuello, A., Queralt, P., Ledo, J., 2005. Applications of dispersion relations to the geomagnetic transfer function. *Phys. Earth Planet. Inter.* 150, 85–91.
- Muñoz, G., 2014. Exploring for geothermal resources with electromagnetic methods. *Surv. Geophys.* 35, 101–122. <http://dx.doi.org/10.1007/s10712-013-9236-0>.
- Nisi, B., Vaselli, O., Tassi, F., Elio, J., Delgado Huertas, A., Mazadiego, L.P., Ortega, M.F., 2013. Hydrogeochemistry of surface and spring waters in the surroundings of the CO₂ injection site at Hontomín-Huermeces (Burgos, Spain). *Int. J. Greenh. Gas Control* 14, 151–168. <http://dx.doi.org/10.1016/j.ijggc.2013.01.012>.
- Ogaya, X., 2014. Magnetotelluric Characterisation and Monitoring of the Hontomín CO₂ Storage Site, Spain (PhD Thesis) Universitat de Barcelona.
- Ogaya, X., Ledo, J., Queralt, P., Marcuello, A., Quintà, A., 2013. First geoelectrical image of the subsurface of the Hontomín site (Spain) for CO₂ geological storage: a magnetotelluric 2D characterization. *Int. J. Greenh. Gas Control* 13, 168–179. <http://dx.doi.org/10.1016/j.ijggc.2012.12.023>.
- Ogaya, X., Queralt, P., Ledo, J., Marcuello, A., Jones, A.G., 2014. Geoelectrical baseline model of the subsurface of the Hontomín site (Spain) for CO₂ geological storage in a deep saline aquifer: a 3D magnetotelluric characterization. *Int. J. Greenh. Gas Control* 27, 120–138. <http://dx.doi.org/10.1016/j.ijggc.2014.04.030>.
- Ogaya, X., Alcalde, J., Marzán, I., Ledo, J., Queralt, P., Marcuello, A., Martí, D., Saura, E., Carbonell, R., Benjumea, B., 2016. Joint interpretation of magnetotelluric, seismic, and well-log data in Hontomín (Spain). *Solid Earth* 7, 1–15. <http://dx.doi.org/10.5194/se-7-1-2016>.
- Park, S.K., 1996. Precursors to earthquakes: seismoelectromagnetic signals. *Surv. Geophys.* 17 (4), 493–516.
- Park, S.K., Dalrymple, W., Larsen, J.C., 2007. The 2004 Parkfield earthquake: test of the 2005 magnetotelluric precursor hypothesis. *J. Geophys. Res.* 112, B5. <http://dx.doi.org/10.1029/2005JB004196>.
- Parker, R.L., 1980. The inverse problem of electromagnetic induction: existence and construction of solutions based on incomplete data. *J. Geophys. Res.* 85 (B8), 4421–4428. <http://dx.doi.org/10.1029/JB085iB08p04421>.
- Parker, R.L., Booker, J.R., 1996. Optimal one-dimensional inversion and bounding of magnetotelluric apparent resistivity and phase measurements. *Phys. Earth Planet. Inter.* 98, 269–282. [http://dx.doi.org/10.1016/S0031-9201\(96\)03191-3](http://dx.doi.org/10.1016/S0031-9201(96)03191-3).
- Patella, D., 1976. Interpretation of magnetotelluric resistivity and phase soundings over horizontal layers. *Geophysics* 41 (1), 96–105. <http://dx.doi.org/10.1190/1.1440610>.
- Peacock, J.R., Thiel, S., Reid, P., Heinson, G., 2012a. Magnetotelluric monitoring of a fluid injection: example from an enhanced geothermal system. *Geophys. Res. Lett.* 39, L18403. <http://dx.doi.org/10.1029/2012GL053080>.
- Peacock, J., Thiel, S., Reid, P., Messellier, M., Heinson, G., 2012b. Monitoring enhanced geothermal fluids with magnetotellurics, test case: Paralana, South Australia. PROCEEDINGS, Thirty-Seventh Workshop on Geothermal Reservoir Engineering, Stanford University, Stanford, California (January 30–February 1, 2012, SGP-TR-194).
- Peacock, J.R., Thiel, S., Heinson, G., Reid, P., 2013. Time-lapse magnetotelluric monitoring of an enhanced geothermal system. *Geophysics* 78, B121–B130. <http://dx.doi.org/10.1190/GEO2012-0275.1>.
- Pellerin, L., Johnston, J.M., Hohmann, G.W., 1996. A numerical evaluation of electromagnetic methods in geothermal exploration. *Geophysics* 61 (1), 121–130.
- Queralt, P., Jones, A.G., Ledo, J., 2007. Electromagnetic imaging of a complex ore layer: 3D forward modelling, sensitivity tests, and down-mine measurements. *Geophysics* 72 (2), F85–F95. <http://dx.doi.org/10.1190/1.2437105>.
- Quintà, A., 2013. El patró de fracturació Alpina en El Sector Suroccidental de Los Pirineos Vascos (PhD Thesis) Universitat de Barcelona.
- Rosas-Carbalal, M., Linde, N., Peacock, J., Zyserman, F.I., Kalscheuer, T., Thiel, S., 2015. Probabilistic 3-D time-lapse inversion of magnetotelluric data: application to an enhanced geothermal system. *Geophys. J. Int.* 203, 1946–1960. <http://dx.doi.org/10.1093/gji/ggv406>.
- Rubio, F.M., Ayala, C., Gumiel, J.C., Rey, C., 2011. Caracterización Mediante Campo Potencial Y teledetección de la Estructura geológica Seleccionada Para Planta de Desarrollo tecnológico de Almacenamiento geológico de CO₂ en Hontomín (Burgos). IGME- Instituto Geológico Y Minero de España Technical Report.
- Sholpo, M.E., 2006. Monitoring of relative changes in the electrical conductivity of rocks from observations of the magnetotelluric apparent resistivity (numerical modelling). *Phys. Solid Earth* 42 (4), 323–329 (ISSN 1069–3513).
- Srivastava, S.P., 1965. Method of interpretation of magnetotelluric data when source field is considered. *J. Geophys. Res.* 70 (4), 945–954.
- Streich, R., 2016. Controlled-Source Electromagnetic Approaches for Hydrocarbon Exploration and Monitoring on Land. *Surv. Geophys.* 37, 47–80. <http://dx.doi.org/10.1007/s10712-015-9336-0>.
- Svetov, B.S., Karinskiy, S.D., Kuksa, Y.I., Odintsov, V.I., 1997. Magnetotelluric monitoring of geodynamic processes. *Ann. Geofis.* XI (2), 435–443.
- Ugalde, A., Villaseñor, A., Gaité, B., Casquero, S., Martí, D., Calahorrano, A., Marzán, I., Carbonell, R., Estaún, A.P., 2013. Passive seismic monitoring of an experimental CO₂ geological storage site in Hontomín (northern Spain). *Seismol. Res. Lett.* 84 (1), 75–84. <http://dx.doi.org/10.1785/0220110137>.
- Vilamajó, E., Queralt, P., Ledo, J., Marcuello, A., 2013. Feasibility of monitoring the Hontomín (Burgos, Spain) CO₂ storage site using deep EM source. *Surv. Geophys.* 34, 441–461. <http://dx.doi.org/10.1007/s10712-013-9238-y>.
- Wagner, F.M., Günter, T., Schmidt-Hattenberger, C., Maurer, H., 2015. Constructive optimization of electrode locations for target-focused resistivity monitoring. *Geophysics* 80 (2), E29–E40. <http://dx.doi.org/10.1190/GEO2014-0214>.
- Ward, S.H., Hohmann, G.W., 1988. Electromagnetic theory for geophysical applications. In: Nabighian, M.N., Corbett, J.D. (Eds.), *Electromagnetic Methods in Applied Geophysics: Theory, SEG Monograph Vol. 1*, pp. 131–313.
- Weidelt, P., 1972. The inverse problem of geomagnetic induction. *Z. Geophys.* 38, 257–289.
- Weidelt, P., Kaikkonen, P., 1994. Local 1-D interpretation of magnetotelluric B-polarization impedances. *Geophys. J. Int.* 117, 733–748. <http://dx.doi.org/10.1111/j.1365-246X.1994.tb02466.x>.